Lab on a Chip

Advances in Microfluidic Platforms for Tumor Cell Phenotyping: From Bench to Bedside.

Journal:	*Lab on a Chip*
Manuscript ID	LC-CRV-05-2024-000403.R1
Article Type:	Critical Review
Date Submitted by the Author:	21-Aug-2024
Complete List of Authors:	Joshi, Rutwik; Texas Tech University, Department of Chemical Engineering Ahmadi, Hesaneh; Texas Tech University, Department of Chemical Engineering Gardner, Karl; Texas Tech University, Department of Chemical Engineering Bright, Robert; Texas Tech University Health Sciences Center, Department of Immunology & Molecular Microbiology Wang, Wenwen; Huazhong University of Science and Technology, Department of Obstetrics and Gynecology, Tongji Hospital, Tongji Medical College Li, Wei; Texas Tech University, Department of Chemical Engineering

Advances in Microfluidic Platforms for Tumor Cell Phenotyping: From Bench to Bedside

Rutwik Joshi [a], Hesaneh Ahmadi [a], Karl Gardner [a], Robert K. Bright [b], Wenwen Wang [c], Wei Li[a]*

a Department of Chemical Engineering, Texas Tech University, Lubbock, TX 79409

b Department of Immunology & Molecular Microbiology, School of Medicine & Cancer Center, Texas Tech University Health Sciences Center, Lubbock, TX 79430

c Department of Obstetrics and Gynecology, Tongji Hospital, Tongji Medical College, Huazhong University of Science and Technology, Wuhan, Hubei, China, 430030

Corresponding Author: wei.li@ttu.edu

Abstract

Heterogeneities among tumor cells significantly contribute towards cancer progression and therapeutic inefficiency. Hence, understanding the nature of cancer through liquid biopsies and isolation of circulating tumor cells (CTCs) has gained considerable interest over the years. Microfluidics has emerged as one of the most popular platforms for performing liquid biopsy applications. Various label-free and labeling techniques using microfluidic platforms have been developed, the majority of which focus on CTC isolation from normal blood cells. However, sorting and profiling of various cell phenotypes present amongst those CTCs is equally important for prognostics and development of personalized therapies. In this review, firstly, we discuss the biophysical and biochemical heterogeneities associated with tumor cells and CTCs which contribute to cancer progression. Moreover, we discuss the recently developed microfluidic platforms for sorting and profiling of tumor cells and CTCs. These techniques are broadly classified into biophysical and biochemical phenotyping methods. Biophysical methods are further classified into mechanical and electrical phenotyping. While biochemical techniques have been categorized into surface antigen expressions, metabolism, and chemotaxis-based phenotyping methods. We also shed light on clinical studies performed with these platforms over the years and conclude with an outlook for the future development in this field.

Table of Contents

1. Introduction

Cancer is the second leading cause of death around the world, only behind cardiovascular diseases [1] and 90% of all cancer related mortalities are caused by metastasis [2]. Metastasis is a process in which the primary tumor releases cancer cells into the circulatory system and these cells travel through the bloodstream and eventually invade distant organs and tissues to form a secondary tumor [3]. These cells released from the primary tumor are defined as circulating tumor cells (CTCs). Presence of CTCs in bloodstream is believed to be the reason for hematogenous spread of cancer [4]. As an alternative to invasive biopsies which can only provide a static "partial photograph" of the tumor mass at that point of time [5], CTCs isolated from blood (liquid biopsy) can be used for early diagnosis, prognosis and monitoring of cancers [6] which can provide a dynamic picture of disease progression.

However, CTCs are present at very low frequencies, as low as 1 to a few in 1 billion cells in patient blood, which poses an enormous challenge in their isolation [7]. There are many isolation techniques which exploit biophysical properties for CTC enrichment like difference in density (centrifugation) [8], size/deformability (microfiltration) [9], hydrodynamics (inertial focusing) [10, 11], and surface conductivity (electrophoresis) [12]. Also, several immunoaffinity based methods are available which use protein expression on the cell surface to capture CTCs using specific antibodies. The CellSearch® system is approved by the US Food and Drug Administration (FDA) for CTC isolation from peripheral blood for analysis. It targets the epithelial cell adhesion molecule (EpCAM), a protein which is overexpressed on the surface of many cancer cells and CTCs, using magnetic particles anchored with anti-EpCAM antibodies. The cells captured are identified as cancer cells using fluorescent cytokeratin antibodies [13].

Although CTC presence in the blood can be a good indicator of disease progression and therapeutic outcomes [14], it does not take into account the heterogeneity of the cancer cell population. CTCs consist of several subtypes, and every subtype exhibits different biophysical and biochemical properties [15]. Heterogeneity among CTCs may be one of the reasons why the molecular profiles of the primary tumor and secondary tumors are not always similar [16, 17]. This heterogeneity in CTCs is displayed in terms of cell surface morphology, metabolic activity, rate of proliferation, protein expression, migration and metastatic potential [18]. Out of these CTC subtypes only a few actually participate in metastasis process [19] as many CTCs are eliminated by the immune system or by the hemodynamic forces [20]. However, some subtypes can survive these forces and escape the immune system to keep on circulating until they extravasate into some distant tissue and form a secondary tumor. In addition, some subtypes may show resistance to certain anti-cancer agents which can be a major factor for inefficiencies of targeted therapy [21].

Intravasation or shredding of cancer cells from primary tumor can occur due to molecular transitioning of cells, known as the epithelial to mesenchymal transition (EMT). Hence, this process plays a vital role in metastasis [22]. During the EMT, the expression level of epithelial cell markers like EpCAM, E-cadherin decreases and the expression level of mesenchymal markers like N-cadherin, Vimentin go up [23, 24]. This transition increases the motility of tumor cells in turn making them more invasive and prone to form metastatic lesions [25]. Similarly, the mesenchymal to epithelial transition (MET) allows the cancer cells to regain their epithelial properties which is believed to be the reason for stabilization of secondary tumors [26]. Tracking these changes and heterogeneity in the cell genotype and phenotype is necessary not only to monitor the disease progression and make decisions about the treatment regimen, but also for the design of new chemotherapeutic drugs and therapies specific to some resistant subtypes.

In order to understand the molecular heterogeneity of cancer cells in individual patients, development of new techniques for CTC capture and subtype identification is critical. There have been many studies on such techniques using microfluidic manipulations and immunostaining methods [27, 28] and new techniques are being developed every year. In this review we will shed light on recent techniques developed for CTC capture, subtype identification and clinical aspects associated with those techniques. We will also provide a brief overview on how these techniques can help decode molecular heterogeneity associated with cancer progression.

The workflow of CTC phenotyping is as follows - First step is the isolation and non-invasive release of cancer cells and CTCs from various samples such as liquid biopsies (blood draw) from cancer patients, or a mixture of cancer cell lines with heterogeneous characteristics spiked into healthy blood. Step two is phenotyping of isolated cancer cells or CTCs. Finally, step three represents the clinical translation in terms of survival rate, chemotherapeutic response and treatment guidance for personalized medicine according to the detected biophysical and biochemical heterogeneities. In this review, our primary focus is on microfluidic platforms for cancer cells and CTC phenotyping.

In section 2, we introduce methods of isolation and non-invasive release of cancer cells and CTCs for downstream analysis. In section 3, we provide a detailed discussion on heterogeneity in cancer cell phenotypes and microfluidic techniques for unravelling those heterogeneities in samples made by spiking cancer cells in healthy blood as a simplified model to mimic CTCs. We also broadly classify these heterogeneities and microfluidic phenotyping techniques into biophysical and biochemical. In section 4, we discuss studies using clinical-relevant samples, such as cancer patient blood, tumor tissue biopsy, mouse xenograft, etc. In addition, we summarize some recent effort on the correlation between CTC heterogeneities and drug response in cancer patient samples. Finally,

we discuss some potential directions for advancing the field of CTC profiling for the growing clinical demands.

2. Isolation and release of tumor cells and CTCs for downstream analysis

Capture, isolation and enumeration of CTCs is an important step in cancer detection and therapeutic outcome in clinical set up. CTC isolation techniques can be evaluated using parameters such as capture efficiency, capture purity, throughput and viability [29]. However, considering the low frequency of CTCs in patient blood, their non-destructive release after isolation is equally vital for downstream characterization and heterogeneity detection. Releasing CTCs captured using size-based isolation by reverse flow has been explored but shear stress affects the viability of fragile CTCs. Hydrodynamic forces and interfacial tension created by air bubble can overcome force of immunoaffinity based capture, however this technique also had drawbacks such as low release efficiency and cell damage [30]. Over the years to overcome these challenges and release captured CTCs in a more gentle and efficient way to preserve their genetic and functional characteristics, microfluidic devices coated with stimuli responsive biomaterials functionalized with CTC specific antibodies for affinity-based capture have been developed [31].

Aptamers, nucleic acids which can bind to cell ligands similar to antibodies have been grafted on microfluidic devices for CTC capture, which can be degraded for non-invasive release by changing their conformation using nuclease mediated degradation[32, 33]. Microfluidic devices coated with electrically stimulated and pH-sensitive materials for CTC capture and release have also been exploited in recent years [34, 35]. Herringbone microfluidic devices coated with various stimuli responsive biomaterials such as nanoparticle binding and ligand exchange [36], enzymatically

degradable layer-by-layer [37], temperature responsive and mechano-sensitive [38] have been widely used for isolation and release of CTCs for downstream heterogeneity analysis. Polyethylene glycol brushes grafted along with antibodies on a herringbone device have also been explored for high purity CTC capture and release [39].

Along with these stimuli-responsive biomaterials based microfluidic platforms, technologies with high throughput fluorescence imaging with nanoliter scale drop dispensation for non-invasive single rare cell isolation, such as Cellenion and SEED Biosciences, have also been developed and commercialized recently. These approaches for CTC isolation and non-invasive release are instrumental for phenotyping and downstream cell analysis since output of these methods in some cases is used as the input for phenotyping.

3. Heterogeneities among tumor cell phenotypes and microfluidic techniques for phenotyping

CTCs have a high degree of heterogeneity among them [40]. This heterogeneity can be in terms of biophysical features like, deformability, adhesion to the surface under shear forces, electrical polarizability, etc., or biochemical characters like genetic and surface antigen expression, metabolism, migration in response to chemoattractant, etc. These differences in cellular characteristics can be indicators of disease progression and drug response and help in designing personalized cancer therapies. In this section, we will discuss heterogeneity among different types of cancer cells and how they are related to aggressiveness of cancer and its progression. A general overview of cancer cell heterogeneity was illustrated in Figure 1. To exploit these heterogeneities, numerous microfluidics platforms have been developed in the recent past which will also be discussed below. Some of these studies provide proof-of-concept for tumor cell phenotyping using

phosphate-buffered saline (PBS) and healthy blood samples spiked with various cancer cells which is a simplified model to actual tumor biopsies and CTCs. Nevertheless, these studies still show a promise for clinical translation to process actual cancer patients blood samples or tumor biopsies for phenotypic profiling after further improvements. An overview of various microfluidic device setups used for cancer cell phenotyping was summarized in Table 1. List of cancer cell lines and clinical samples used for CTC phenotyping/profiling along with the method of microfluidic phenotyping and biomarkers targeted for profiling was listed in Table 2. In the clinical translation section (section 4), a few studies which demonstrate the ability of microfluidic devices to profile CTC phenotypes with cancer patient blood samples [41-43] and mouse xenografts [44] will also be discussed.

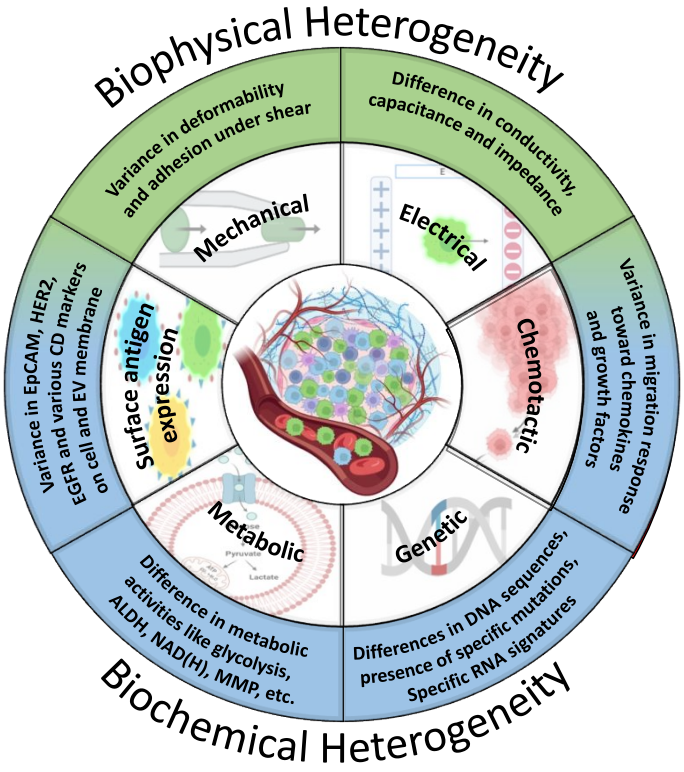

Fig 1. – General overview of cancer cell heterogeneity: Classification of heterogeneities among CTC phenotypes into biophysical and biochemical heterogeneities. Created with Biorender.com.

Table 1 – Overview of various microfluidic device setups used for cancer cell phenotyping –

Phenotyping Principle	Microfluidic Setup	Ref.
Mechanical Profiling	Consecutive constriction channel with ionic current detection	62, 70
	DLD triangular micropillars & rectangular microarray	63
	Elasticity microcytometer: Parallel tapering funnel-shaped confining channels	65, 71
	Bottleneck constriction channel	66
	Oval shaped microbarriers & propeller microstructure	44
Electrical Profiling	Electromicrofluidic chip with gold electrodes	81
	Constriction channel with four electrodes	82
	Cytological slide chip with AC electric field	83
Surface antigen-based sorting with IMNP	2-tier magnetic sorter device	91
	X-shaped pillars with linear velocity valleys	92-99
	Microfluid bins with magnetic gradient	100
	Magnetophoretic device with vanadium Permedur strips	101
	Tassel-shaped trapezoidal micropillars	104
Surface antigen-based profiling without IMNP	DLD architecture with triangular micropillars	106, 107
	Herringbone channels in series	108
Chemotactic Profiling	V-shaped geometry & microchannel network	114
	Triangular microposts with migration channel	113
	Horseshoe-shaped microwells	116
Metabolic Sorting	Serpentine channel & inertial focusing with pulsed electric field	125
	Droplet microfluidics	126, 127
	Vortex trapping & droplet microfluidics	128

**DLD – Deterministic Lateral Displacement, *IMNP – Immunomagnetic Nanoparticles*

3.1.Biophysical Heterogeneity

Cancer cell biomarkers like genetic profile layout and protein expression are pivotal in early identification of cancer and to asses disease progression [45]. These biochemical differences also

translate into changes in biophysical properties of cells which can also be used to identify cancer cells and their phenotypes for monitoring disease progression. Mechanical properties like deformability, detachment under shear forces, stiffness, etc. differ with cancer cell phenotype transition and stage of the disease [46]. Electrical properties like crossover frequency, cell membrane capacitance and membrane potential have also been observed to be different for benign and aggressive cancer stage as well as for different cancer cells [47, 48]. Similarly, cancer cell phenotypes also have different optical properties like refractive index and light scattering [49, 50]. All these biophysical properties mentioned above can be used for early cancer detection, monitoring its progression and taking decisions about changing treatment course. In the following sections, we will discuss these biophysical heterogeneities in cancer cells for phenotype identification.

3.1.1. Mechanical Heterogeneity and Mechanical Phenotyping

It is a well-known fact that cancer cells show heterogeneity among themselves in terms of cellular stiffness and deformation [51]. Along with deformability, the ability of different cancer cell phenotypes to adhere to surfaces under shear forces also shows variations and can be used as a general marker to identify metastatic cells [52]. Metastatic cancer cells are highly motile, invasive and have five times lower stiffness than that of benign cells having low motility and invasiveness [53, 54]. Hence, variations in mechanical properties of cancer cells are good tools to identify phenotypes of cells present in the tumor. Atomic force microscopy (AFM) [55], magnetic tweezers [56], micropipette aspiration [57], deformability cytometry [58], basic cell adhesion assays [59], are some of the commonly used techniques which are used to measure cancer cell deformability and adhesion. This type of heterogeneity among cancer cells and extracellular matrix surrounding them arises due to the alterations in cytoskeletal elements of cells, like actin, microtubules and

actomyosin [60, 61]. As mentioned above, there are some techniques available to measure these mechanical properties of cells, however their low throughput and need of sophisticated equipment hinder their widespread application. Development of high throughput, cost-effective and easy to use techniques to quantify cancer cell mechanical properties is essential.

Changes in cytoskeletal structure of cells induce alteration in mechanical properties of cancer cells as the disease evolves with time. Microfluidic devices with various geometries are ideal tools to evaluate this potential by measuring properties like deformability, stiffness and adhesion under shear forces. Most of the studies dealing with CTCs only take into consideration the mechanical differences between cancer and normal blood cells, but there have been some studies which explore the differences between various cancer cell phenotypes, including cancer stem cells (CSCs). In this subsection, we will summarize some of these studies.

Sano *et al*. used a microfluidic device with ionic current detection and two consecutive constrictions for simultaneously measuring cell size and deformability of HeLa cells, both untreated and treated with different anti-cancer drugs to check the effects of drugs on their deformability. The inlets and outlets of this device were connected to a constant electric field and ionic current measuring device as depicted in Figures 2A (I) and (II). Signal intensities of the changes in ionic current when the cell passed through the front constriction gave the cell volume and diameter, while the residence time of the cell at the rear constriction was interpreted as a measure of the deformability of cells. The authors studied the effect of two different anti-cancer drugs, Latrunculin A (0.5 μM) and Paclitaxel (50 nM) on HeLa cells after 2h of treatment. They found that the size of untreated and treated cells was the same. Latrunculin A treated cells had a shorter residence time in the rear constriction as compared to that of the untreated cells as depicted in graphs in figures 2A (III) and (IV), while Paclitaxel treated cells had a slightly longer residence

time than to that of the untreated cells. These results suggested a difference in mechanism of action of the two drugs [62].

Liu and co-workers developed a high-throughput microfluidic cytometry device to isolate rare cancer cells based on their size and further characterize those based on their transportability through micro-constrictions, as depicted in Figure 2B-(I). Stiffness and the frictional property of cell while passing through constrictions were the parameters used to determine transportability of cells. An invasive phenotype might be indicated by lower cell stiffness and surface friction force and was predicted by a higher transportability score, which is inversely proportional to elastic modulus and the friction coefficient [63]. The authors evaluated transportability of breast epithelial cell lines which included normal epithelial breast cells (MCF10-A), luminal breast cancer cells (MCF-7 and SKBR-3) and triple negative breast cancer cells (MDA-MB-231, SUM149 and SUM159). Triple negative cell lines showed higher transportability and heterogeneity than luminal cell lines (Figure 2B-(II)). The effect of tumor promoter, 12-O-tetradecanoylphorbol-13-acetate (TPA), on MCF-7 cells was also evaluated by the authors. TPA treated MCF-7 cells showed higher transportability than untreated MCF-7 cells (Figure 2B-(III)). This suggested alterations in adhesion protein expression and cell structure by TPA. Along with these *in-vitro* cell culture studies, the authors looked at heterogeneity in mouse tumor xenografts using the same device, which will be discussed in the section on the clinical aspects.

Park *et. al.* developed a dual mechanical AFM-based technique to assess the enhanced mechanical conformity and cell substrate adhesion of metastatic breast (MCF-7 and MDA-MB-231) and prostate cancer cells (CL-1 and LnCaP) [64]. The results showed a strong correlation between mechanical conformity and metastatic potential for breast cancer cell lines. The elastic modulus of MDA-MB-231 cells, which are highly metastatic, was found to be significantly higher than MCF-

7 cells, which have much lower metastatic potential. A reverse relationship was observed in the case of prostate cell lines. Results of cell-substrate adhesion test of prostate cancer cells demonstrated higher adhesion of CL-1 than LnCaP, indicating a direct relationship between cell-substrate adhesion and metastatic potential, however this correlation was not observed with breast cancer cells. From these results the authors concluded that using dual mechanical signatures (elasticity and cell-substrate adhesion) can be correlated with different types of cancer cells and their metastatic potential. Although these results have significance in correlating mechanical properties with metastatic potential of tumor cells, use of AFM would not be practical in current clinical setting, considering the low number of CTCs in patient blood, low throughput, high cost and time associated with AFM operation.

Hu and coworkers developed an elasticity microcytometer for dual mechanical and biochemical profiling of cancer phenotypes [65]. Using this device, the authors profiled cell size and cell deformability along with surface antigen expression. For this purpose, they used parallel tapering channels with entrance and exit widths as 32μm and 6μm respectively with uniform height of 40μm (Figure 2C-(I)). Cells originating from different tissues like normal breast (MCF-10A), breast cancer (MCF-7), cervical cancer (HeLa) and prostate cancer (PC3) were profiled using this multiparametric approach. Cell deformability was measured at 100Pa inlet pressure and was significantly lower for non-malignant MCF-10A cells as compared to all other cancer cells (Figure 2C-(II)). For profiling EpCAM expression, the same device was coated with anti-EpCAM antibodies and cells were injected into the device at 100Pa pressure for 2-5 minutes to ensure antigen-antibody interactions. To quantify expression levels by adhesion force of antigen-antibody interactions, inlet pressure was gradually increased with an increment of 1000Pa over time. PC3 and MCF-7 (Figure 2C-(III)) cells required significantly higher pressures to flush the cells out of

channels as compared to MCF-10A and HeLa cells (Figure 2C-(IV)), confirming their high EpCAM expression based on higher adhesion force.

In another study, N. Liu and coworkers developed a morphological rheological microfluidic device to study differences in mechanical properties of androgen non-sensitive (PC3 and DU145) and androgen sensitive (LnCaP) prostate cancer cells [66]. For this purpose, they used a bottlenecked microfluidic channel and a contour extraction method for image processing and data analysis (Figure 2D-(I)). Using this technique, the degree of deformation of androgen sensitive LnCaP was found to be higher than androgen non-sensitive PC3 and DU145 cells (Figure 2D-(II)). The AFM results indicated that the Young's modulus of androgen non-sensitive cells was higher than androgen sensitive cells (Figure 2D-(III)), and that difference in mechanical properties of prostate cancer cells can be used as a marker to predict androgen sensitivity.

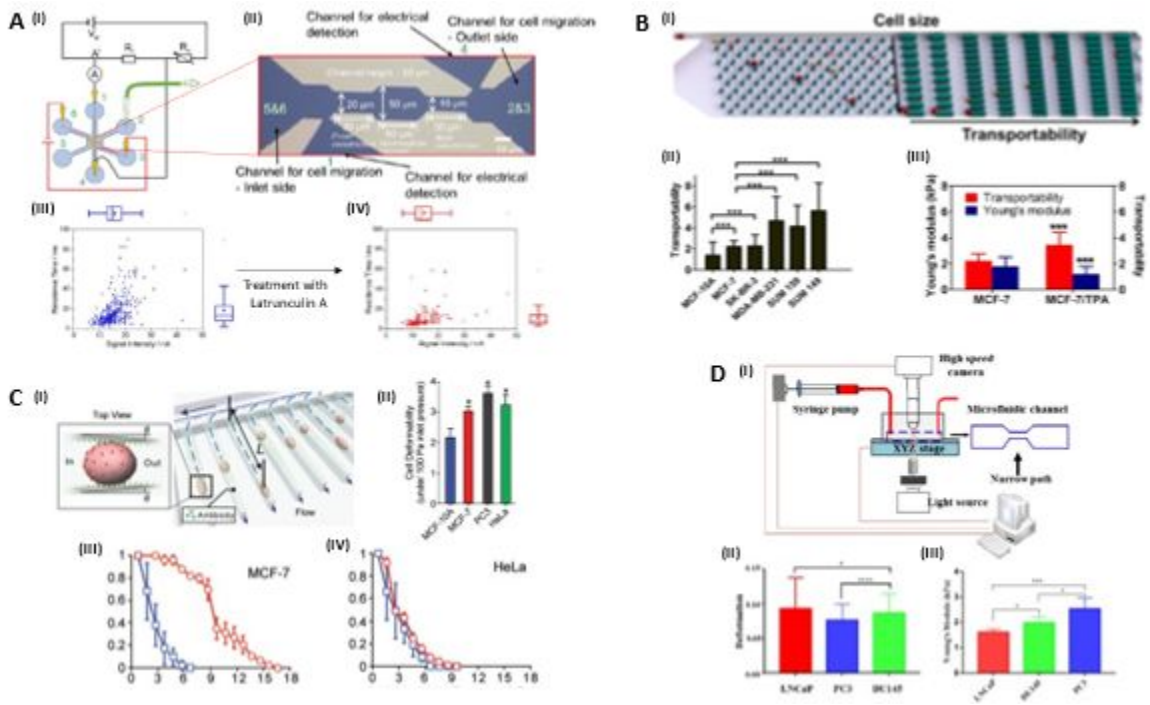

Fig 2. – Mechanical phenotyping methods: (A) (I) Schematic of the microfluidic set up with a constant electric field applied between openings 3 and 6 (in red), an external electric circuit to detect changes in current during cell passage between 1 and 4 (in black) and a pump connected at 2 (in green) in withdraw setting to drive the cells through the

constriction coming in from inlet numbered 5. (II) in-set is the microscopic image of the constriction channel with dimensions. (III) The residence times of the HeLa cells without latrunculin A (N = 317, blue dots) and (IV) after treatment with latrunculin A (N = 149, red dots) at the rear constriction as a function of signal intensity. Reproduced with permission from ref [62]. Copyright (2019) American Chemical Society **(B)** (I) Schematic of the deterministic lateral displacement (DLD) on the left for size-based separation and a trapping barrier microarray on the right for determination of transportability of different types of cancer cells. (II) Average transportability of 6 different breast cancer cell lines (MCF-10A, MCF-7, SK-BR-3, MDA-MB-231, SUM 159 and SUM 149). (III) Comparison of Young's modulus determined by AFM and transportability of TPA treated and untreated MCF-7 cells. Data are presented as mean ± s.d. ***P < 0.001. Reproduced with permission from ref [63]. Copyright (2015), Springer Nature **(C)** (I) Schematic of the elasticity microcytometer with a linearly decreasing width from inlet channel width of 32μm to 6μm at the outlet. L is the distance travelled by the cells in the channel under a constant inlet pressure which is the measure of cell size and deformability, while θ is the slant angle created by the narrowing channels (inset). Inset figure represents the antibody coated channel which is useful for determining the surface protein expression level, number of covalent bonds and bond strength between antigen and antibody for different cancer cell lines (II) cell deformability of 4 cancer cell lines. (MCF-10A, MCF-7, PC3 and HeLa) under a constant inlet pressure of 100 Pa. (III) Fraction of live single cancer cells remaining trapped in confining channels of the elasticity microcytometer (y-axis) as a function of additional hydraulic pressure applied to flush out cancer cells from confining channels (x-axis in kPa). Confining channels were either coated with pluronics F-127 (control, blue) or antibodies against EpCAM (red). Reproduced with permission from ref [65]. Copyright (2016) Wiley-VCH GmbH **(D)** (I) Schematic of the workflow of the developed method. (II) Average degree of deformation of 3 prostate cancer cell lines of interest (LnCaP, DU145 and PC3) and (III) Young's modulus of prostate cancer cells using AFM. Reproduced with permission from ref [66].

3.1.2. Cancer Stem Cells (CSCs) and CSCs Identification

In the heterogeneous cell population of tumors there is a subpopulation of cells which express the surface biomarkers CD44, CD24 and CD133, possess self-renewal properties, and show chemotherapeutic resistance. In addition, this cell subpopulation plays a significant role in cancer metastasis and post treatment relapse, and are referred to as cancer stem cells (CSCs) [67]. These cells also have characteristics of being highly deformable with low adhesive properties [68, 69]. CSCs have distinct mechanical properties from other cancer cells which make them more invasive. Identification of these aggressive subpopulations is very important for better treatment outcomes. There have been several studies on sorting and profiling of CSCs using microfluidic devices, which will be discussed below.

Sano *et al.*'s work discussed earlier was continued by Terada *et al.* with slight modifications in the device geometry to develop a label-free assay for detection of CSCs [70]. The width of rear constriction was optimized to 6μm to get higher range of residence times for different types of

cells and all other dimensions were kept unchanged (similar to schematic in Figure 2A-(I and II)). Size and deformability of HT29, Caco2, HeLa, MDA-MB-231 and Jurkat cells were measured. HT29 and Caco2 cells showed the highest amount of heterogeneity in deformabilities, as evidenced from normalized residence time plots depicted in Figure 3A-(I). HT29 cells were sorted using fluorescence activated cell sorting (FACS) based on aldehyde dehydrogenase (ALDH) activity and sorted cells were analyzed for deformability using the microfluidic device. Normalized residence time was found to be 4.9 ± 3.8 and 2.7 ± 1.5 seconds for high ALDH activity of cells and low ALDH activity cells, respectively (Figure 3A-(II)).

Work from Hu *et al.* on elasticity microcytometer discussed earlier was continued by Chen *et al.* to explore biophysical phenotypes of inflammatory breast cancer (IBC) stem like cells [71]. In this study, the authors identified distinct biophysical and survival properties of ALDH+ subpopulation of IBC cells which are highly metastatic and tumorigenic. To prove differences in ALDH+, a prominent CSC marker, and ALDH- phenotypes, an invasiveness assay with Matrigel was performed which proved highly invasive behavior of ALDH+ subpopulation of IBC cells, SUM149. For biophysical phenotyping, an elasticity microcytometer was used with single cells in each tapering channel (Figure 3B-(I)). ALDH+ subpopulation of SUM149 showed increased deformation capabilities (Figure 3B-(II)), which may help them to squeeze through tight junctions of endothelial cells initiating metastasis. This correlated cytoskeletal changes in cells with the stemness marker ALDH+. In the second part of this study, the authors evaluated the adhesion capabilities of two subpopulations under shear forces in a microfluidic channel (Figure 3B-(III)). ALDH+ cells demonstrated lower adhesion strength (Figure 3B-(IV) and (V)) which indicated the reason for their migration away from primary tumor and causing metastasis.

Jia and coworkers designed a microfluidic tandem mechanical sorting device for isolation of CSCs from heterogeneous cancer cell populations by exploiting their higher deformability and low adhesion strength in a single device (Figure 3C-(I)) [44]. The mechanical sorting chip (MS-chip) had eight microchannels with two million oval micro posts with 7μm distance in between. While the high throughput adhesion chip (HCA-chip) was made with propeller microstructures and coated with basement membrane extract to mimic *in-vivo* conditions. The lung cancer cell line A549 was used for *in-vitro* sorting experiments. Cells sorted with the MS-HCA-chip showed higher stemness markers including CD133, CD44, SOX2 and β-actin (Figure 3C-(II)). This correlated with higher chemotherapeutic resistance, increased cell proliferation (Figure 3C-(III) and higher spheroid formation capabilities (Figure 3C-(IV)), as compared to those for unsorted (sort-in) cancer cell populations.

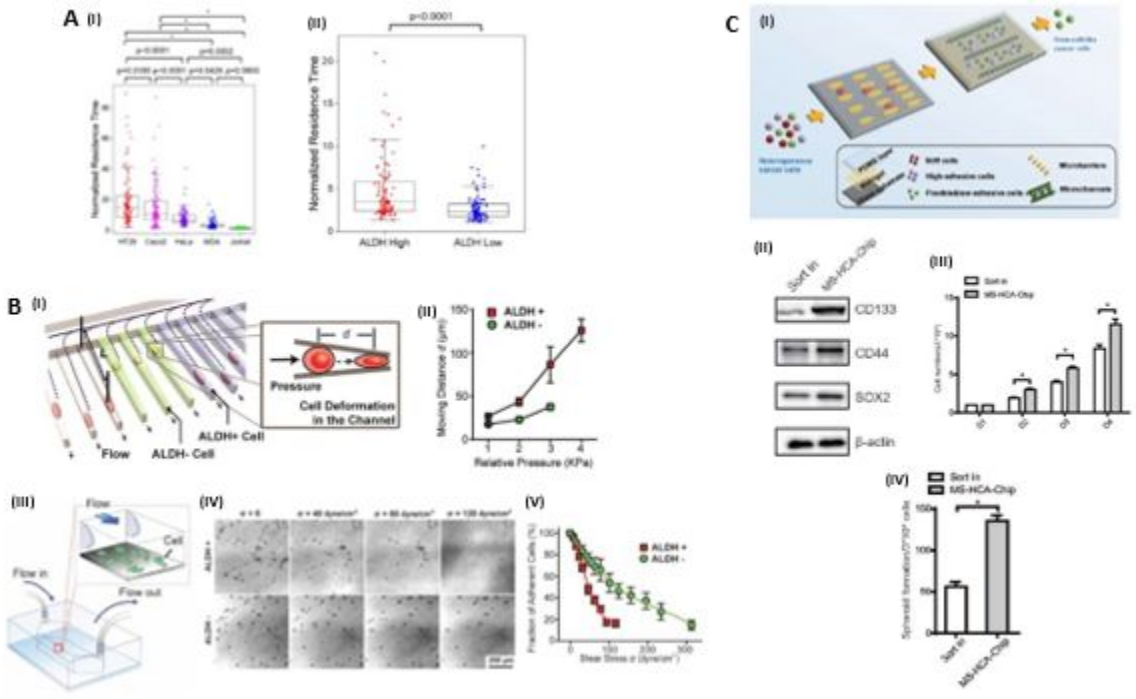

Fig 3. – Sorting and Identification of cancer stem cells: (A) (I) Normalized residence time performed using two consecutive constrictions with 6μm rear constriction for mechanotyping of HT29, Caco2, HeLa, MDA-MB-231, and Jurkat cells. (II) Normalized residence times of HT29 cells sorted according to ALDH activity using FACS for mechanotyping based on stemness character. The measurements were performed at following conditions: RPMI at

room temperature, 3 V for electrophoresis, and 3 μL/min for hydrodynamic flow. Reproduced with permission from reference [70]. Copyright (2021) American Chemical Society. **(B)** (I) Schematic of microfluidic deformability microcytometer for single cell deformability measurements. (II) Differential penetrating distances under various pressures for ALDH+ and ALDH- SUM149 cells in the deformability microcytometer. (III) Schematic of a microfluidic channel for quantification of cell adhesion strength under continues fluid shear. (IV) Brightfield images showing detachment of ALDH+ and ALDH- SUM149 cells from the microfluidic channel with increasing fluid shear stress. (V) Fraction of ALDH+ and ALDH− SUM149 cells remaining adherent in the microfluidic channel after 3 minutes of continues fluid shear. Reproduced with permission from ref [71]. Copyright (2019) Wiley-VCH GmbH **(C)** (I) Schematic illustration of the integrated microfluidic MSHCA- chip for collection of stem cell-like cancer cells with high flexibility and low adhesion. (II) Western blot analysis showing expression levels of different stemness markers among sort in and MS-HCA-Chip sorted cells. (III) Different growth rates of sort in and MS-HCA-Chip sorted cells over a period of 3 days. The same number of cells from both groups were plated in 6-well plate and number of cells were counted every day. (IV) Quantification of spheroid formation of spheroids derived from sort in and MS-HCA-Chip separated cells. Reproduced with permission from ref [44]. Copyright (2021) Wiley-VCH GmbH.

In summary, advanced mechanical phenotyping methods to identify metastatic cancer cells like mesenchymal cells and CSCs have been developed to investigate cell deformability and surface adhesion strength differences in heterogeneous cancer cell population. Exploiting these differences can be used for sorting aggressive phenotypes like mesenchymal CTCs and CSCs, and to identify potential mechanical features of highly metastatic cancer cell subpopulations. These techniques help researchers understand how metastatic cancer cells escape from the primary tumor and squeeze through tight junctions of blood vessels to enter the circulation and spread to distant organs and tissues.

3.1.3. Electrical Heterogeneity and Electrical Phenotyping

Electrical properties of cancer cells are indicators of cell membrane structure and cytoplasmic contents or composition of particular type of cells. Differences in dielectric properties of cancer cells also contribute to inter and intra tumoral heterogeneity as different cancer cell subpopulations show different polarizabilities. It has been observed that roughness, protein glycosylation and protein concentration affect dielectric properties of cells [72, 73]. Crossover frequency is defined as the frequency at which the cell membrane and the cell medium have the same polarizability and the cell remains stationary [74]. Crossover frequency depends on the conductivity of cell medium

and cell membrane capacitance as well as the cell's internal dielectric properties [75]. It has been observed that the aggressiveness of cancer cells and their crossover frequency have an inverse relationship [76]. Electrical properties of cancer cells are influenced by biomarker expressions and the microenvironment of cells. For example, more metastatic cancer cells have higher the ionic marker Na^+/H^+ Exchanger 1 expression level, migration potential, conductivity, and permittivity [77]. Electrical cell impendence sensing [78] and dielectrophoresis (DEP) [79] are the two most common techniques employed in measuring dielectric properties of cancer cells. Coupling these with microfluidics can improve high-throughput analysis. Distinct phenotypes may be sorted or identified by exploiting differences in their dielectric properties from a cancer cell mixture. Electrical characteristics like conductivity, permittivity, membrane capacitance and impedance are analyzed to detect heterogeneous subpopulations using different device assemblies. In this section, we will discuss some of the recently developed techniques to identify cancer phenotypes using electrical methods.

Dielectrophoresis (DEP) is a simple technique which can be employed for rapid and label-free detection, characterization and/or sorting of different cancer cells. Vaillier and coworkers developed a microfluidic system to differentiate between an array of cell lines originating from different organs and different stages of cancer by electrical monitoring (Figure 4A-(I)) [76]. The Clausius-Mossotti factor (Re[CMF]) was utilized for the expression of electrode configuration and electric field applied to mobilize the cells electrically [80]. The authors compared the normal prostate cell line RWPE-1 with cancerous prostate cell lines PC3 and LnCaP. The average frequencies recorded for these cell lines were 25±2, 8±1 and 5±3 kHz respectively (Figure 4A-(II)). The authors also recorded crossover frequencies of RWPE-1 and tumorigenic cell lines NA22, NB11 and NB26 that display increasing invasiveness. These cell lines were made

tumorigenic by exposing RWPE-1 cell line to N-methyl-N-nitrosourea (MNU) for different time intervals. It was observed that NA22, NB11 and NB26 had decreasing average crossover frequencies of 12±1, 6±1 and 4±1 kHz, respectively (Figure 4A-(III)). This indicated an inverse relationship between cancer aggressiveness and crossover frequency, which may be attributed to changes in protein expression and morphology of cell membrane during carcinogenesis.

Zhou *et al.* used dual biophysical characterization of cell deformability and electrical impedance of undeformed and deformed cells, which may provide enhanced distinction between cancer cell phenotypes than single marker characterization [81]. In this study, the authors studied biophysical properties of MCF-7 cells and phorbol 12-myristate 13-acetate (PMA) modified MCF-7 cells (modMCF-7). PMA was used as a tumor promoter to alter the properties of MCF-7 cells and form an invasive subpopulation [82]. A differential impedance measurement scheme was used with 4 pairs of electrodes throughout the microfluidic constriction device (Figure 4B-(I)). It was demonstrated that it was difficult to distinguish between different subpopulations of MCF-7 cells from single marker (either passage time through constriction alone or only impedance alone), as there was considerable overlap between their properties. However, while using both markers at the same time, in case of deformed cells traveling through constriction, a clear divide between impedance (Figure 4B-(II)) and transit time in constriction (Figure 4B-(III)) of MCF-7 and modMCF-7 cells was observed. This result suggested that PMA treatment made MCF-7 cells more invasive by changing its mechanical and electrical properties.

Jahangiri and coworkers employed a low frequency AC electric field (1kHz – 200kHz) for polarization of cancer cells based on their metastatic potential and achieved electrical phenotypic cell sorting in a microfluidic device [83]. Non-cancerous breast cell MCF-10A and cancerous breast cells with varied aggressiveness, MCF-7, MDA-MB-231 and MDA-MB-468, were used for

analyzing device performance. The schematic of the microfluidic device used is depicted in Figure 4C-(I). At a particular frequency, cells start to align and get entrapped near the cathode. Increase in frequency diminishes that effect and cells are released from the cathode. This frequency is called "characteristic polarizability frequency" (CPF). MCF-10A showed CPF of 160kHz and MCF-7, MDA-MB-231 and MDA-MB-468 showed CPF of 140kHz, 70kHz and 40kHz, respectively (Figure 4C-(II) and (III)). With these results, the authors concluded that CPF decreases with an increase in the aggressiveness of cancer cells.

In another study, Wang *et al.* studied the relation between conductivity (σ) and permittivity (ε) of breast cancer cells with tumor microenvironment and biomarker expression at different states of malignancy [77]. MCF-10A, MCF-7 and MDA-MB-231 were used as model cell lines. MDA-MB-231 showed higher cell suspension and cell medium conductivity and permittivity than that of MCF-7 cells (Figure 4D-(I) and (II)). MDA-MB-231 also showed higher expression of ionic marker NHE1, which is a key H^+ transporter in breast cancer cells, along with higher cell migration rate. These results established an important relation between the difference in biomarkers between primary (MCF-7) and metastatic (MDA-MB-231) breast cancer cells and their electrical properties.

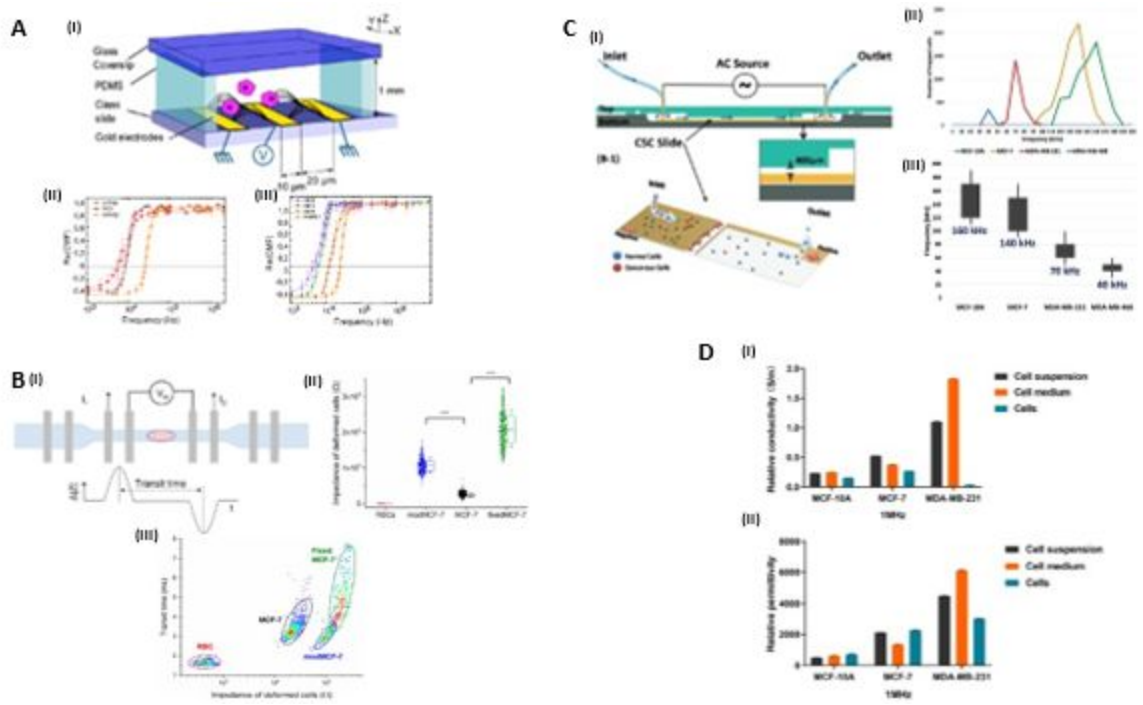

Fig 4. – Electrical phenotyping methods: (A) (I) Cross-section view of the chip in which gold electrodes are attached to a glass slide. Cell suspension is then filled in the PDMS channel before covering it with a coverslip and AC current application (II) Clausius-Mossotti factors vs frequency plots for cell lines RWPE-1 (noncancerous epithelial cells), PC3 and LnCaP (epithelial cells from prostate carcinoma) and (III) The family of tumorigenic MNU cells (NA22, NB11, NB26) and RWPE-1. Reproduced with permission from ref [76]. Copyright (2016) American Chemical Society. **(B)** (I) Electrode connection for the measurement of transit time inside the constriction. (II) Impedance of fully deformed cells inside the constriction measured at the frequency of 1 MHz. (III) Transit time vs impedance of deformed cells inside the constriction. Reproduced with permission from ref [81]. Copyright (2018) American Chemical Society. **(C)** (I) Representation of setup to create electric field gradient by applying AC signal to the electrodes at inlet and outlet of the assembly and 3D schematic of the AC cytological slide chip (AC-CSC) used for polarizing and trapping cancer cells in the active area created by AC electric field. (II) Number of cells from 4 different breast cancer cell lines (MCF-10A (non-cancerous), MCF-7, MDA-MB-231 and MDA-MB-468) trapped at different AC electric frequencies. (III) Frequency response range for different breast cancer cell lines and the ideal polarizing frequency for each cell line. Reproduced with permission from ref [83]. Copyright (2020) Royal Society of Chemistry. **(D)** Comparison among the (I) conductivity (σ) and (II) permittivity (ε) of the three types of cells, cell media, and cell suspensions at 1 MHz. Reproduced with permission from ref [77]. Copyright (2021) Springer Nature.

In summary, recently developed electrical phenotyping methods have demonstrated their effectiveness in distinguishing various subpopulations of cancer cells. All these methods are label-free and low cost, and the samples can be reused for further analysis as they are not destroyed in the process. All the features make electrical phenotyping an attractive field to explore and with

further advancements, this technique has a potential to identify aggressive CTC subpopulations with high precision.

3.2.Biochemical Heterogeneity -

Biophysical changes in cancer cells take place due to biochemical factors like genetics and protein expression of cells. These biochemical changes lead to differences in biophysical properties of different phenotypes of cancer cells through alterations in cytoskeletal architecture as mentioned in the previous section. But biochemical differences alone, like gene expression, surface protein expression, chemotactic migration, cell metabolism can also be exploited for profiling and identifying molecular makeup of the tumor. In this section, we will discuss the biochemical heterogeneity associated with different phenotypes of cancer cells.

3.2.1. Heterogeneous Surface Protein Expression and Surface antigen expression-based phenotyping

Differences in surface protein expression of cancer phenotypes is the most explored feature in understanding cancer heterogeneity. EMT, as explained earlier, plays a major role in cancer metastasis as the epithelial markers are down regulated and mesenchymal markers are up regulated during this transition. EpCAM is the most widely studied surface biomarker as nearly 70% of all cancer cell subtypes express it at different levels [84]. But apart from EpCAM, huma epidermal growth factor receptor 2 (HER2) and epidermal growth factor receptor (EGFR) are also abundantly present in some tumor types [85] and are attractive targets for surface biomarker profiling. SKBR3, an epithelial breast cancer cell line exhibits high HER2 and EpCAM expression with moderate expression level of EGFR [86], on the other hand MDA-MB-231, a highly mesenchymal breast

cancer cell line exhibits low EpCAM and HER2 but has high EGFR expression [87]. Along with these, vimentin, E-cadherin and N-cadherin are also important biomarkers associated with EMT of CTCs [88, 89] and hence are also targets of interest. Apart from these surface biomarkers, some specific cancer markers like asialoglycoprotein receptor (ASGPR) which is up regulated in malignant hepatocellular carcinoma [89] and prostate-specific membrane antigen (PSMA) which shows higher expression levels in aggressive prostate cancer [90] are also considered important in decoding cancer heterogeneity. There are a number of techniques like flow-cytometry, microfluidics, fluorescence in-situ hybridization (FiSH) for profiling surface biomarker expressions of different cancer phenotypes. As mentioned previously, microfluidics has been one of the most widely used platforms for cancer cell isolation. But in recent years it has also been applied in biochemical phenotyping of cancer cells, considering the possibility of precise manipulation of fluid flow inside micrometer-size channels and response of different cancer cell subpopulations to those flow conditions. Here we will discuss the microfluidic approaches developed in recent years for tumor cell antigen expression profiling and cell sorting.

3.2.1.1 Immunomagnetic nanoparticle (IMNP) mediated sorting

Tagging cells with antibody coated IMNPs and sorting them magnetically in a microfluidic device based on the level of antigen expression has been the most widely used technique in recent years. Jack et al. used a series of magnetic sorting devices with different separations gaps to sort heterogeneous pancreatic cancer cells tagged with IMNPs into low, medium and high levels of EpCAM expressions [91]. Figure 5A-(I) illustrates the schematic of the device used by the authors. In the first sorter that had a wider gap between waste and collection channels, mixture of cells of all expression levels were infused and only cells with high magnetic labelling were collected, while cells with low and medium labelling went to the waste channel. In the next sorter with narrower

gap, waste from the first sorter was infused and cells with medium labelling were collected in collection outlet and low labelled cells were collected at waste outlet. Figure 5A-(II) shows the histogram of sorted cells with EpCAM fluorescence by FACS and level of bead attachment on sorted cells supporting the claim of efficient sorting.

Kelley's group used a similar approach of nanoparticle tagging with different microfluidic devices having X-shaped pillars to create low velocity zones for capturing and sorting cancer cells [92-95]. The authors used velocity and magnetic field gradients in various studies to create different capture zones based on the level of antigen expressed by different cancer cell lines. This type of zoned sorting of cancer cells was able to indicate the downregulation of epithelial marker (EpCAM) in the process of EMT. In another example, Mohamadi and co-workers made a velocity gradient with four different zones of EpCAM expression by increasing the channel volume (Figure 5B-(I))[96]. Here, velocity in zone 1 was maximum to capture cells with high EpCAM expression and zone 4 had the lowest velocity to capture low EpCAM expressing cells. Each zone had a lower velocity than the previous one by a factor of 2 (Figure 5B-(II)). Cells were captured in each zone when the magnetic force on cells exerted by magnetic field and nanoparticles was higher than drag force created by fluid flow. The authors used VCaP, SKBR-3 and MDA-MB-231 with decreasing EpCAM expression levels (Figure 5B-(III)) and observed VCaP cells primarily in zone 1, SKBR-3 with 10-fold lower EpCAM expression than VCaP in zones 2 and 3 and MDA-MB-231 with lowest EpCAM expression in zones 3 and 4 (Figure 5B-(IV)). Instead of velocity, Poudineh *et al.* employed a magnetic field gradient by linearly increasing diameters of magnets under the X-shaped pillars to capture high EpCAM cells in the earlier zones and low EpCAM cells in the later zones. They used the same model cell lines and observed similar results as the velocity gradient.

[97]. The same group also performed a two-dimensional profiling of cancer cells by profiling EpCAM and HER-2 expression on a similar device by using aptamer coated IMNPs [98].

More recently, Green *et al.* used the combination of circular pillar and X-shaped pillar devices in series for profiling CTC clusters. The clusters and single cells were first tagged with anti-EpCAM antibody and functionalized IMNPs. The circular pillar device had six zones and pillars with increasingly shorter gaps between them along the length to sort clusters according to their size and deformability. Large, cohesive, rigid clusters were trapped in initial zones. Smaller, more cohesive, and more deformable clusters and large single cells got captured in later zones. This allowed profiling based on size and deformability. Highly deformable clusters and smaller single cells which passed through the circular pillar device entered the X-device connected in series and sandwiched between magnets for immunomagnetic capture. The X-device was constructed with eight zones with decreasing velocity profiles for EpCAM profiling, as illustrated in Figure 5C-(I). The authors used four different subpopulations of cancer cells, MDA-MB-231, MDA-ECAD (MDA-MB-231 modified to have higher E-cadherin and EpCAM expression), MCF10DCIS and MCF10DCIS-Mes (with higher mesenchymal properties) for validation. Figures 5C-(II) and (III) depict the results of cell types captured in each zone of two devices in series. The authors were able to demonstrate the effects of E-cadherin and higher mesenchymal characteristics on cluster formation along with collective motility of cells and small differences in epithelial state using this device [99].

In another study by Civelekoglu and co-workers, the authors devised a method to electrically track the trajectories of different breast cancer cells tagged with EpCAM targeted IMNPs in a microfluidic channel under a magnetic field gradient. A total of eight different bins were made at the outlet with increasing magnetic field strength (Figure 5D-(I)) to sort cells with high EpCAM

expression (MCF-7) in lower bins and low EpCAM expressing cells in higher bins (MDA-MB-231). The bin outlets had electrodes for electrical detection of cells passing, and cell types passing through each bin were determined by fluorescent tags (Figure 5D-(II)). Bin 1 and bin 5 showed the maximum number of cells which correspond to low and high EpCAM bins, respectively. Using fluorescence microscopy, it was confirmed that 89.75% of all the cells which passed through bin 1 were MDA-MB-231 and 81.25% of all cells were MCF-7 in bin 5 (Figure 5D-(III)). Authors also demonstrated that changing the flow rate can help in specifically probing only high or only low EpCAM expressing cells [100].

In another study, Williams *et al.* proposed a microfluidic device for sorting immunomagnetically tagged heterogeneous cancer cells according to their EpCAM expression [101]. The authors propose to bond small Vanadium Permendur strips to the outer walls of the device for precise control over cell separation. EpCAM expression levels of different cell lines acquired from Ozkumur *et al.*[102] along with their magnetophoretic mobilities were also mentioned. The authors claimed that the magnetic field gradient applied across the breadth of the channel will separate cell subpopulations based on the difference in their magnetophoretic mobilities created by magnetic tagging [101].

In a more recent study, Zheng et al. reported an ultrasonically activated microfluidic system for continuous modification of nanoparticles [103]. They grafted silica modified Fe_3O_4 nanoparticles with folic acid to capture CTCs through folate receptors. Hela cells with higher expression of folate receptors and A549 cells with low expression of folate receptors were used to confirm the specificity of the mentioned nanoparticles. In the presence of a magnetic field, the capture yield of Hela cells was found to be 89% while it was only 11.8% for A549 cells, demonstrating a significant advantage of modified nanoparticles to capture tumor cells with overexpression of folate receptor.

Lv et al. designed a near-infrared (NIR) light-responsive lateral flow microarray (LFM) chip. The chip was injected with a solution containing gelatin as a temperature-sensitive material and gold nanorod as photothermal material to provide high viability release. The cell-trapping structure comprised tassel-shaped trapezoidal micropillars within the capture unit, two trapezoidal structures with slits were designed to selectively capture relatively large tumor cells (>8 μm) while excluding WBCs and red blood cells. MDA-MB-231, SK-BR-3, and MCF-7 cells were magnetically labeled with Anti-EpCAM-Biotin-Streptavidin-Magnetic Beads. In response to the gradient magnetic field, the majority of MCF-7 cells with the highest expression of EpCAM were captured towards the front of the chip, whereas MDA-MB-231 cells with the lowest expression of EpCAM were captured at the end of the chip. The isolated CTCs can be collected in large quantities under normal body temperature conditions or released using NIR at specific locations. When exposed to 37°C for 15 minutes, 96 ± 4% of the captured cells were released. Likewise, the photothermal selective release method achieved a successful release of 93 ± 2% of the captured cells in the chip [104].

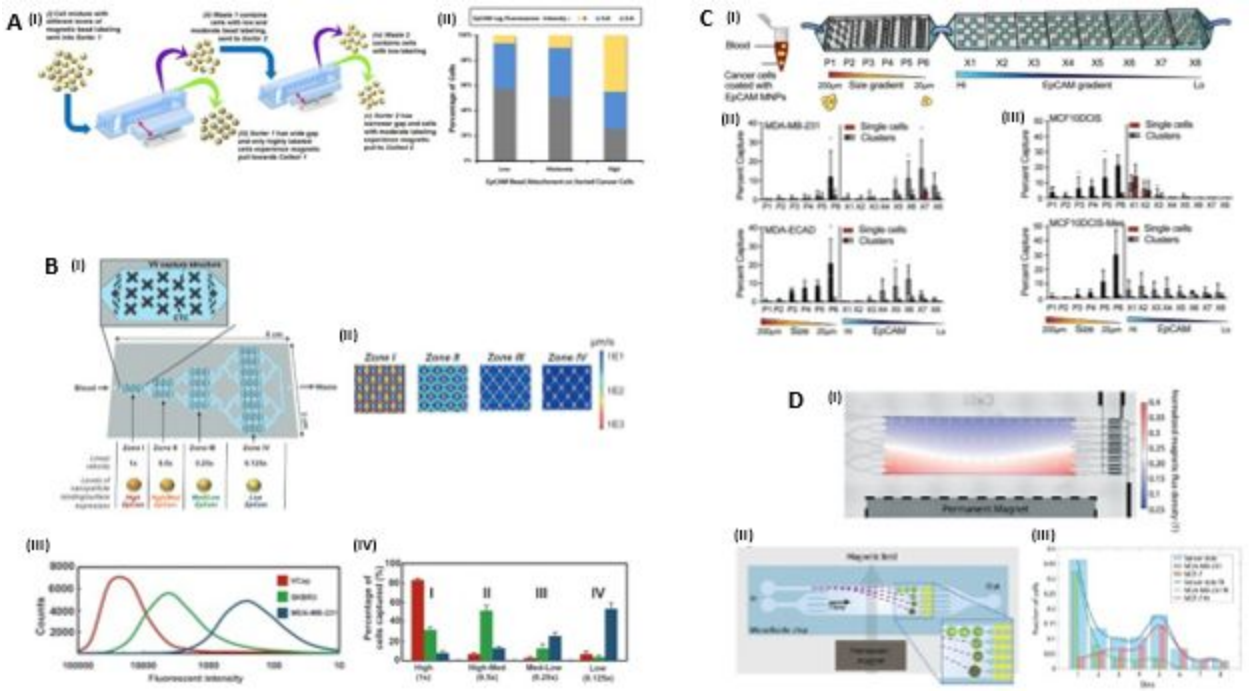

Fig 5. – Profiling surface antigens by immunomagnetic nanoparticle mediated microfluidics: (A) (I) Schematic of 2-tier magnetic sorting process. 3 different cell populations are sorted according to protein expression levels, low, moderate and high respectively. Red arrows indicate separation width between sorter and external magnet. (II) FACS histogram of EpCAM protein expression of PANC-1 cells sorted as low, moderate and high EpCAM expressing cells. Reproduced with permission from ref [91]. Copyright (2017) Royal Society of Chemistry. **(B)** (I) A multizone velocity valley device with four different regions with linearly decreasing velocities (1X, 0.5X, 0.25X and 0.125X). High EpCAM cells will be trapped in zone I, cells with medium and low EpCAM levels being trapped in consecutive zones. (II) Flow profiles for zones I–IV showing the decrease in linear velocity in the different zones. (III) Expression of EpCAM on three cell lines tested using fluorescently labeled anti-EpCAM and flow cytometry. (IV) Distribution of Vcap (red), SKBR3 (green), and MDA-MB-231 (blue) cells in the multizone device. Reproduced with permission from ref [96]. Copyright (2014) Wiley-VCH GmbH. **(C)** (I) Microfluidic device design for capture of CTCs and CTC clusters. Single CTCs and CTC clusters in whole blood are initially labelled with EpCAM specific antibodies conjugated to magnetic nanoparticles. Labeled cells are introduced into the micro-fluidic device at a flow rate of 750 μL h–1. Large and more rigid cohesive clusters are trapped in the Pillar-device consisting of 6 zones (P1-P6), with decreasing pillar gap sizes ranging from 200 to 20 μm. More deformable clusters and single cells pass into the X-device, consisting of 8 zones (X1–X8) containing X-shaped microstructures ranging from 50 to 400 μm in height, which separate cells based on EpCAM expression using the magnetic nanoparticles. (II) PillarX capture profiles of the MDA-MB-231 and MDA-ECAD cells/clusters in the different zones. (III) PillarX capture profiles of the MCF10DCIS and MCF10DCIS-Mes cells/clusters in the different zones. Reproduced with permission from ref [99]. Copyright (2022) Wiley-VCH GmbH. **(D)** (I) Simulated magnetic field due to external magnet inside the microfluidic device. (II) Sheath-flow focused cells deflect in the transverse axis based on their magnetic load under an external magnetic field as they traverse the microfluidic chip. (III) A histogram showing the sorted distribution of 1: 1 mixture of MDA-MB-231 and MCF-7 cells to microfluidic bins. The total number of sorted cells in each bin is obtained electrically. The composition of the sorted population in each microfluidic bin was obtained through fluorescence microscopy. Two sub-histograms represent the fraction of each cell line (green for MDA-MB-231 and red for MCF-7) for each bin. Reproduced with permission from ref [100]. Copyright (2019) Royal Society of Chemistry.

In summary, IMNP mediated techniques are one of the most widely studied in this field. However, use of IMNP comes with the risk of particle internalization which can put cells under considerable stress [105]. There are also some methods which profile cancer cells without magnetic tagging, as discussed in the next subsection.

3.2.1.2.Non-magnetic profiling

In case IMNP mediated capture and profiling, the microfluidic channels are sandwiched between the magnets and the immunomagnetically tagged cells get captured when magnetic field force overcomes the drag force of fluid. For non-magnetic methods, the microfluidic channels are coated with antibodies by different techniques for immunocapture and profiling. The cells are not immunomagnetically pre-tagged and they get captured when the force of antibody-antigen interaction overcomes the drag force and shear created by fluid flow.

Ahmed *et al.* used a size-dictated immunocapture (SDI) device with rotated triangular micropillars coated with anti-EpCAM antibodies (Figure 6A-(I)). The working principle of this architecture is deterministic lateral displacement (DLD), where the cells with larger size like cancer cells, interact more with the micropillars and smaller sized cells pass through with little interaction. The antigen expression of captured cells was profiled utilizing shear force gradients around the pillars created by hydrodynamic flow. Shear force gradients were simulated using computational fluid dynamic software and then matched with experimental conditions for profiling (Figure 6A-(II)). Kato III, SW 480 and HUH7, cancer cell lines with different EpCAM expression were used for validation. Kato III cells, with highest EpCAM expression of all, got captured mostly at high shear stress regions (around the triangle tips) as their antigen-antibody bond strength was high enough to overcome high shear forces. While SW 480 and HUH7 with relatively lower EpCAM expression got captured in the low shear regions around the pillars (Figure 6A-(III)). The authors claimed that

this method allowed them to estimate the antigen expression of the captured cancer cell just by its capture position [106].

This work was continued by Zhu and co-workers, where they attempted to profile surface antigen of hepatocellular carcinoma cells (HCC) using in combination two different antibodies, anti-EpCAM and anti-ASGPR, in parallel identical SDI channels as depicted in Figure 6B-(I) [107]. Human hepatoma cell lines HuH-7 and SK-HEP-1 which express both EpCAM and ASGPR antigens and human acute lymphoblastic leukemia cell line CCRF-CEM which does not express either EpCAM or ASGPR (confirmed by flow cytometry), were used for validation. The capture efficiency of anti-EpCAM and anti-ASGPR was found to be 89 and 85% for HuH-7 and SK-HEP-1 cells, respectively. CCRF-CEM only showed 6 and 5% capture in two channels which was attributed to non-specific binding (Figure 6B-(II) and (III)). By this the authors confirmed identification of HCC cells from heterogeneous mixture of other cancer cells.

Wang *et al.* constructed an assembly of microfluidic devices for combined enrichment, capture and phenotypical sorting by epithelial and mesenchymal biomarker expression of breast cancer cell lines MCF-7 and MDA-MB-231. The phenotypical sorting was achieved by two herringbone channels in series with different antibodies coated on each. The first channel was coated with anti-EpCAM antibodies for capturing cells with epithelial traits, while the second channel was coated with a cocktail of Axl, PD-L1 and EGFR antibodies for capturing cells with mesenchymal traits (Figure 6C-(I)). After the capture, 88.4±2.7% of the total captured cells in anti-EpCAM region were MCF-7, while only 10.2±1.1% were MDA-MB-231. In the triple antibody region, 80±2.1% of the total captured cells were MDA-MB-231, while only 3±0.9% were MCF-7 (Figure 6C-(II)). This ensured differential capture and phenotyping of cancer cell characteristics without immunofluorescent labelling of cells. The authors also managed to culture the captured the cells

in the microfluidic device and release them with high viability for further downstream analysis [108].

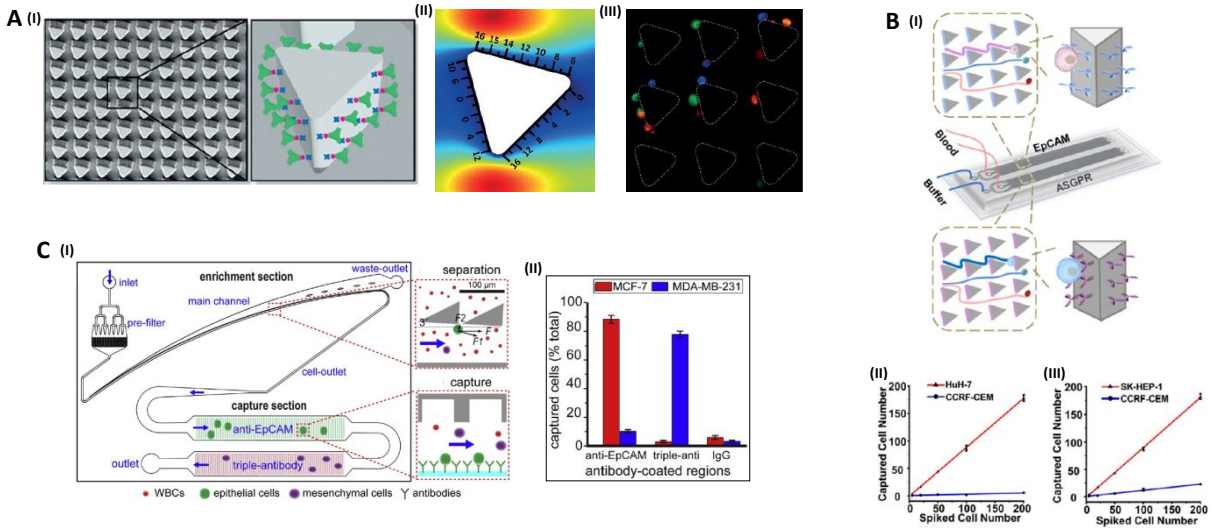

Fig 6. – Profiling surface antigens by antibody-coated microfluidic channels: (A) (I) SEM image of triangular microarray structures (left), and diagram demonstrating antibodies immobilized on the surface of each micropillar (right). (II) Shear stress gradient (dyn/cm2) of fluid flow around the triangular micropillar. (III) Micro-graph depicting the distribution of captured cells based on EpCAM expression level around micropillars (cells were labeled with Vybrant multicolor cell labeling kit before mixing and capture, blue = KATO III, red = HUH7, green = SW480). Reproduced with permission from ref [106]. Copyright (2017) Wiley-VCH GmbH. **(B)** (I) Schematic of the synergetic chip for heterogeneous CTC capture and phenotypic profiling. (II) Capture efficiencies of the anti-EpCAM antibody modified channel and (III) the anti-ASGPR antibody modified channel in PBS buffer. Reproduced with permission from ref [107]. Copyright (2020) American Chemical Society. **(C)** (I) Schematic illustration of the enrichment and the capture sections of the device; the separation of tumor cells and WBCs by crossflow filtration and the specific capture of tumor cells on the antibody-coated substrate. (II) Differential capture of MCF-7 and MDA-MB-231 cells (1:1 ratio) in the capture section. Reproduced with permission from ref [108]. Copyright (2021) Elsevier.

3.2.2 Chemotactic Heterogeneity and Chemotaxis-based Phenotyping

Chemotactic migration of adherent cells is one the rate-limiting factors in metastasis development [109]. Chemotaxis is stimulated by chemoattractants like chemokines and growth factors which are detected by chemokine receptors present on membranes of cancer cells [110, 111]. Heterogeneity is observed among CTCs from patients with respect to their response to

chemoattractants and the cells which are more prone to chemotaxis are believed to contribute in metastatic process [112]. It has been observed that cancer cells having mesenchymal characteristics show higher chemotactic migration as compared to those having epithelial characteristics [113]. This behavior of mesenchymal cells resembles their character of being highly invasive and metastatic. There are various microfluidic techniques that have been developed to study this heterogeneous property of cancer cells and exploit it for phenotypic profiling, as discussed below.

H. Zou and coworkers designed a microfluidic device capable of generating multiple serum gradients to study the difference in chemotactic migration behavior between lung cancer stem cells (LCSCs) and differentiated LCSCs (dLCSCs,16^{th} passage of LCSCs). Figure 7A-(I) shows the schematic of the microfluidic device with two inlets and one outlet used for this study. Fetal bovine serum (FBS) was used as a chemoattractant at various concentrations to make gradients. 24h after loading the cells in the gradient chip, LCSCs showed slower migration potential than dLCSCs to serum gradient stimulus (Figure 7A-(II) and (III)). This indicated plasticity of cancer cells, as LCSCs and dLCSCs came from the same origin, but dLCSCs changed over time during 16 passages of *in-vitro* culture. Migration response after drug treatment of both types of cells was also recorded and drug treatment resulted in lower migration rates of LCSCs and dLCSCs. Even after drug treatment, dLCSCs had faster migration rates than LCSCs. This platform provided a novel approach of studying chemotaxis and drug response of different cancer cell phenotypes [114].

Poudineh *et al.* first sorted prostate cancer cells PC3 and LnCaP according to EpCAM expression by tagging with aptamer functionalized MNPs using a microfluidic device with X-shaped pillars. The sorted cells were released for profiling their migratory response to CXCL16 gradient, a prostate cancer cell migration inducing chemokine. A chemotaxis chip was designed with

triangular microposts near the channel inlet for cell trapping (Figure 7B-(I)). The Chemokine concentration was low at the inlet and increased along the channel. Migration distances were measured at 0, 5, 10, 15 and 20h for both the cell lines. PC3 cells, which are more invasive and mesenchymal than LnCaP cells, migrated faster over greater distance than LnCaP (Figure 7B-(II) and (III)). This supported the conclusion that LnCaP cells do not respond to chemoattractant and mesenchymal phenotypes like PC3 cells, which have higher migration potential than epithelial phenotypes[113].

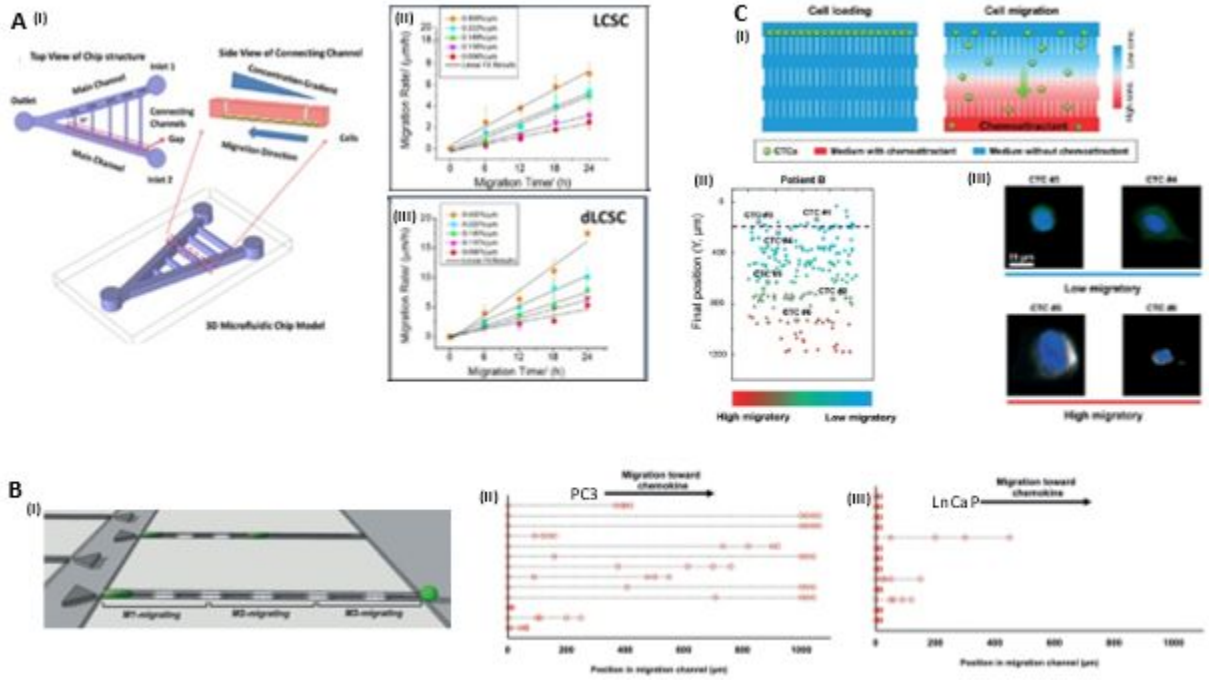

Fig 7. – Profiling chemotactic response and migration: (A) (I) The microfluidic chip with two main channels forming a 30° V-shaped structure and five parallel connecting channels with different lengths. Cells migrate in direction of chemoattractant gradient. The increasing (II) LCSCs and (III) dLCSCs migration rates in channels at different local serum concentrations in the gradients. Reproduced with permission from ref [114]. Copyright (2015) American Chemical Society **(B)** (I) The cell loading channel connected to the chemoreservoir through the migration channels. Cells migrate from the cell-loading channel to the chemoattractant reservoir. The migration channel divided into three regions (M1, M2 and M3) to study the migration of different cell subpopulations more effectively. (II) PC3 migration monitored at different time points: 0 h, 5 h, 10 h, 15 h, and 20 h after cell loading. The position of 13 cells measured at each time point. Each red circle denotes the cell position at one time point. (III) LNCaP migration observed at different time points. Reproduced with permission from ref [113]. Copyright (2016) Wiley-VCH GmbH. **(C)** (I) Cells loaded into the top microchannel at the beginning of the migration assay. A gradient of growth factors established over a 24-hour period through continuous flow to let cells to migrate to different distances and at different speeds depending on their phenotypes. The direction of the arrow indicates the gradient of the growth factors. (II) Migration distance of CTCs (n = 207) from patient blood sample. Cells were loaded into the migration device at the

same starting position (dashed line, Y = 200 μm). (III) Immunofluorescence images of low migratory cells (top, found close to the loading channel of the migration device) and high migratory cells (bottom, found in the migration channels of the device). Reproduced with permission from ref [115]. Copyright (2021) Royal Society of Chemistry.

In a more recent study, Lu et al. designed a cascaded microfluidic chip that integrates a spiral structure for CTC separation from whole blood. They also incorporated a single-cell array structure consisting of horseshoe-shaped microwells for in-situ molecular and functional heterogenicity analysis. EpCAM and Vimentin expression of SGC-7901 cells, A549 cells, and HT-29 cells were measured in the single-cell array. Based on fluorescence intensity and quantitative results it was observed that these cell lines displayed reduced EpCAM and increased vimentin fluorescence signals with the order being HT-29 cells, A549 cells, and SGC-7901 cells. This pattern correlated with an elevated metastasis potential. Moreover, the dynamic invasion behavior of cells induced by FBS concentration gradient was observed for 24 hours. Their motility trajectories, and velocities were analyzed to reflect cell motility function. HT-29 cells were primarily concentrated within the microwell. SGC-7901 cells exhibited a more dynamic mobility, while A549 cells displayed a moderately mobile behavior. This system provides a potential approach for real-time monitoring of a single CTC's behavior change, showing the functional heterogeneity of CTCs [116].

In summary, Chemotactic potential is an important biochemical property of cancer cells as it indicates the metastatic potential and drug response. There are few other studies that deal with chemotactic phenotypes of cancer cells, which have been discussed elsewhere [117-119]. Continuous efforts are being made to further demystify this using microfluidics combined with other advanced technologies.

3.2.3 Metabolic Heterogeneity and Metabolism-based Phenotyping

Metabolic activities of cells vary depending on their phenotypic state. Cancer cells are metabolically heterogeneous is a well-established fact [120]. These metabolic differences between various cancer cell phenotypes arise from intrinsic factors such as cell lineage, differentiation state, somatic mutations, as well as from properties of the tumor microenvironment such as availability of nutrients, interactions with stromal cells and extracellular matrix [120]. High metabolic heterogeneity exists between different types of tumor cells and therapies targeted towards metabolic pathways can show reduced efficiency due to this heterogeneity [121]. Factors which induce EMT in cancer cells can also alter metabolic pathways and induce upregulation of glycolysis in cells going through the transition [122]. A study from Schwager et al. [123], unveiled this phenomenon after phenotypic sorting of highly and weakly migratory cancer cells. While highly migratory cells with mesenchymal properties use glycolysis, cells with epithelial and weak migration properties use mitochondrial respiration for glucose metabolism. Other than glycolysis, high ALDH activity is also an indicator of tumor initiation and metastatic cancer cell subtypes [124]. Higher collagen digestion ability is an indicator of mesenchymal phenotype cells which are highly invasive and higher nicotinamide adenine dinucleotide phosphate (NADPH) metabolism is also linked to an invasive cell subtype [94]. These metabolic heterogeneities have been combined with modern techniques like microfluidic and fluorescence microscopy to identify metastatic cancer cell subpopulations, which will be discussed in this section.

D. Feng and co-workers used a serpentine device to attain continuous cell separation and inertial focusing along with a pulsed electric field-induced electrospray ionization-high resolution mass spectrometry (PEF-ESI-HRMS) for single cell analysis. Pulsed square wave electric field was utilized for online recognition of cell disruption and induction of electrospray ionization (Figure

7A-(I)). They achieved a throughput of 80 cells/min and detected and profiled around 120 metabolites in a single cell. Three thousand MCF-7 and HepG2 cancer cells were analyzed and their metabolic profiles were used to differentiate between two cell types using principal component analysis (Figure 8A-(II)). Outliers among the same types of cells were detected using a machine learning technique called Isolated Forest and the probability of finding outliers came out to be around 5% (Figure 8A-(III)). This technique provided a high throughput method of metabolic profiling and identification of cancer cell phenotypes based on mass spectrometrically extracted metabolomics [125].

It is noted that metabolic differences result in varied pH in cellular microenvironment. Pan *et al.* exploited this effect by single cell encapsulation using droplet microfluidics. Droplets were sorted as live/dead cells, based on the difference in their pH and interfacial tension as an effect of differential cellular lactate release into the droplet microenvironment [126]. This technique was called sorting by interfacial tension or SIFT as the droplets with lower pH resulting in lower interfacial tension, which were separated by upward ride on the rail in the microfluidic device (Figure 8B-(I)). This work was continued by Zielke *et al.* to sort cancer cells with high and low glycolytic activity. Malignant cancer cells with high glycolytic activity resulted in droplets with higher pH microenvironments, while non-malignant cancer cells exhibited lower pH droplets. Hypoxic conditions, which trigger higher rates of glycolysis were simulated by treating MDA-MB-231 cells with $CoCl_2$. K562 cells treated with 2-deoxy-D-glucose (2DG), a drug that targets cell metabolism, were also used to verify the effect of this drug on cellular glycolysis. Both types of treated and untreated cells were efficiently separated using SIFT. Figures 8B-(II) and (III) show the distribution of treated and control MDA-MB-231 cells after sorting with SIFT. The SIFT method successfully sorted malignant cancer cells based on single cell glycolytic activity

differences. This was an inexpensive and easy technique which can be used without tagging the cells [127].

Matrix metalloproteases (MMPs), proteolytic enzymes secreted by cells for ECM protein breakdown, play a major role in CTC invasion into surrounding tissues resulting in metastasis. Invasive cancers have shown increased levels of MMPs through immunohistochemistry. This characteristic high secretion of MMPs was used by Dhar *et al.* to identify aggressive phenotypes in different lung (A549 and HCC827) and prostate (VCaP, LnCaP and PC3) cancer cells. The authors developed a process of size-based isolation by vortex trapping and subsequent single cell encapsulation using a microfluidic droplet generator in pristine fluorogenic reporter solution for measuring MMP secretion by individual cells (Figure 8C-(I) and (II)). Figure 8C-(III) shows the fluorescence intensity in droplets encapsulated with different cell lines after 3h, varying levels of MMP secretions were observed from various cell lines highlighting metabolic heterogeneity [128]. Protease activity in cells isolated from patient blood was also analyzed, which will be discussed in section 4.

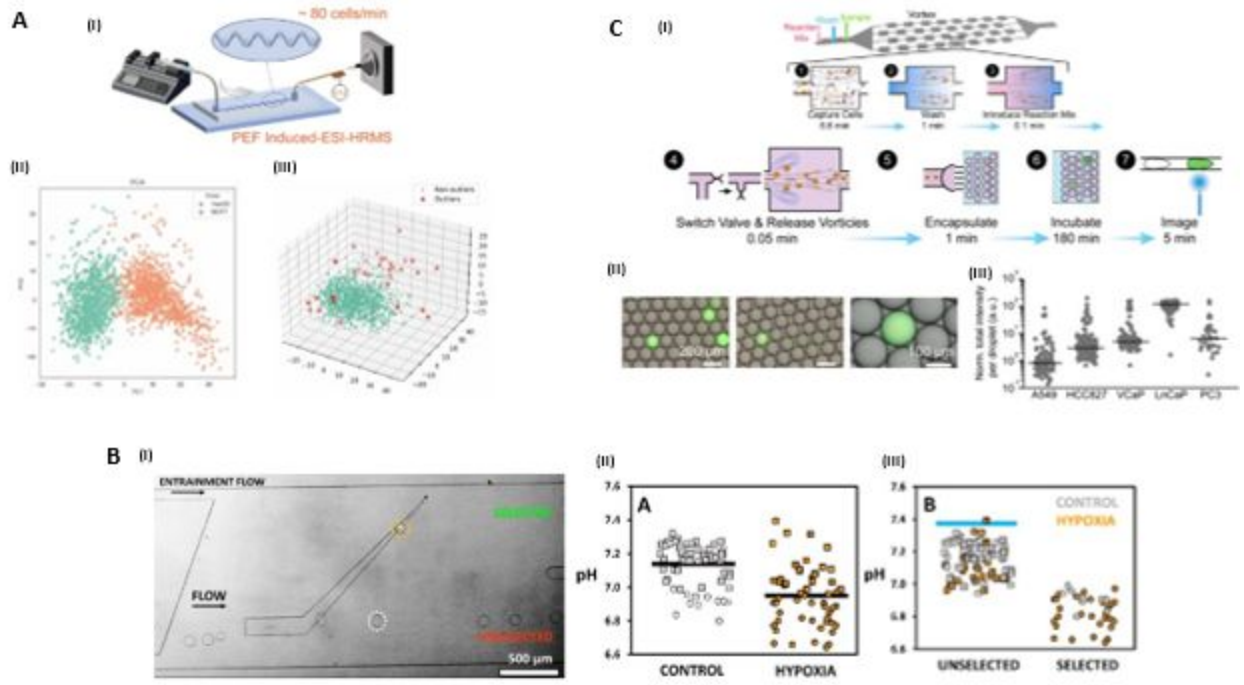

Fig 8. – Identification by metabolic activity: (A) (I) Schematic diagram of the microfluidics chip assisted high-throughput single cell mass spectrometry analysis device. (II) PCA plot based on the first two principal components of the single HepG2 and MCF7 cells. (III) Outliers in HepG2 cells (marked by red x in 3D PCA plot) identified by Isolation Forest. Reproduced with permission from ref [125]. Copyright (2022), Elsevier. **(B)** (I) Image of the SIFT device separating hypoxic and normal MDA-MB-231 cells. Droplets containing cells treated with CoCl2 (hypoxic) and grown at lower pH are selected and get deflected by the rail because of higher glycolysis levels, while droplets containing cells grown under normal conditions do not get deflected by the rail. (II) and (III) Cells grown under normal conditions or control (grey), cells grown under hypoxic conditions (orange), selected droplets (circles) and unselected droplets (squares). The mean pH of control and hypoxic droplets is represented by the black lines while the blue line marks the mean pH of empty droplets. Reproduced with permission from ref [127]. Copyright (2020), American Chemical Society **(C)** (I) Size-based purification and encapsulation of cells (SPEC) followed by fluorescence analysis of enzyme secretion (1). Large cells get trapped in microvortices, while smaller cells and molecules are washed away with a wash buffer (2). An MMP-cleavable peptide substrate solution is introduced through another fluid exchange (3). Vortices are dissipated by lowering the flow rates and captured cells are released into the substrate solution. A pinch valve is opened to the droplet generator in synchrony with vortex dissipation (4). The droplets float away from the droplet generator due to buoyancy differences with the oil (5). The cells are then incubated and imaged in the large reservoir section. An imaging cytometer can also be used to image the droplets and contained cells in flow (6 and 7). (II) fluorescence of only droplets with single viable cells was measured, and intensity normalized as a ratio of empty drop levels. (III) MMP secretion levels vary across cell lines. Lung cancer cell lines (A549 and HCC827) and prostate cancer cell lines (VCaP, LnCaP, and PC3) secrete varying levels of MMPs. Reproduced with permission from ref [128]. Copyright (2018) National Academy of Science.

3.2.4 Genetic Heterogeneity

There have been studies that indicate considerable inter and intra-tumoral heterogeneity in gene expression [129]. Genetic instability among cancer cells translates into higher somatic abnormalities which leads to mutations. These mutations give rise to heterogeneity which is responsible for phenotypic variations and hinderance with development of personalized treatments as it may lead to drug resistance [130, 131]. Aggressiveness of cancer can be predicted by up and down regulation of some of the expressed genes. Yu *et al.* and co-workers proposed a 70-gene "aggressiveness predictor model" for prostate cancer. In this study they mapped the expression levels of 70 genes of different prostate cancer patients and predicted if the disease was aggressive or non-aggressive from the gene expression profile [132]. RNA sequencing and quantitative real-time reverse-transcription PCR (qRT-PCR) are the most commonly used techniques for quantification of gene expressions, but the more challenging part is analyzing those results to arrive at a conclusion.

In recent years circulating tumor DNA (ctDNA) has also shown great potential as a heterogeneity biomarker for real-time diagnosis and prognosis of cancer [133]. ctDNA is released into the blood stream from primary tumor lesions, micrometastatic lesions, CTCs after an event of apoptosis or necrosis [134]. ctDNA and CTC profiling are complementary to each other[135], even though ctDNA is more abundant than rare CTCs in blood and can also be obtained from liquid biopsies. ctDNA has demonstrated promise in cancer heterogeneity detection[136], genomic evolution of cancer at various stages during therapies and resistance development mechanism through extensive sequencing [137, 138]. Along with ctDNA, cell free miRNA (cfRNA) and extracellular vesicles (EVs) have also gained significant attention as liquid biopsy analytes in clinical settings [139, 140]. Analyzing data from such multitude of analytes (CTCs, ctDNAs, cfRNA and EVs) will

require coupling sequencing with machine learning tools such as logistic regression and neural networks [141] for improved performance and decision making. Heterogeneity among surface protein expression of EVs is beyond the scope of the current manuscript and it has also been discussed elsewhere [142, 143].

4 Clinical Translation to Tumor Biopsies and CTCs

Development of new methods for biophysical and biochemical phenotypic profiling of CTCs is essential to understand characteristics of different cancer cell phenotypes in a rapid and low-cost way. However, demonstrating the efficiency of these methods and devices in clinically relevant samples is equally important for solving real-world problems. Although there are several research groups which have managed to develop novel phenotypic profiling methods, examples of their translation to clinical samples are currently limited. Depending on the clinical status of the patients and the locations of tumor lesion, solid biopsy of tumor tissue might not be feasible at all instances. Furthermore, sampling from a single location of tumor tissue might not capture the heterogeneities involved in the disease. Hence, liquid biopsies which can capture multitude of tumor associated analytes such as CTC, CTC derived exosomes and ctDNA through a simple blood draw have become favorable alternatives to solid biopsies [144]. In this section we will discuss some of the microfluidic CTC biomarker profiling efforts which have proved clinical translatability with tissue biopsies and liquid biopsies. We will also shed some light on how different heterogeneities among CTCs and tumor masses may affect the survival rate, drug response or develop resistance to certain drugs.

4.1 Biophysical Heterogeneity

As mentioned earlier, mechanical properties of CTCs also play a pivotal role in their migration, drug response and survival. EMT induces major cytoskeletal changes in CTCs which leads to changes in stiffness and malignant transformation [145]. Different CTC subpopulations derived from various cancer types have shown distinct response to fluid shear stress in blood circulation, i.e. higher stiffness of CTCs lead to lower cell viability and vice versa [146]. These characteristics of CTCs have been exploited in some clinically relevant studies which will be discussed here.

The clinical and drug screening potential of a microfluidic tandem mechanical device for sorting CSCs was reported by Jia *et al.* using xenograft models with A549 tumor bearing mice [44]. A natural flavonoid derived from licorice called ISL, with reported tumor progression suppressing properties was tested for its CSCs targeting properties. MS-HCA-chip sorted A549 cells were subcutaneously injected into mice and the mice were treated with ISL in PBS every other day, while control groups were treated with PBS alone. Tumor volume and weight of mice from each group were recorded after sacrificing the mice post 28 days. Both tumor volume and weight of sorted A549 cells injected mice treated with ISL were significantly lower than the control group treated with PBS. More importantly, tumor volume and weight of mice injected with MS-HCA-chip sorted A549 cells, which had more stem characteristics after treatment with ISL, was significantly lower than the control group. This proved the ability and efficacy of ISL in targeting CSCs.

Along with microfluidic devices, AFM has emerged as a tool to assess biomechanical parameters of CTCs such as elasticity, deformation and adhesion. Pawel Osmulski and co-workers used AFM-based nanomechanical characterization to detect castration resistant prostate cancer (CRPCa) in CTCs from patient samples. Elasticity, deformation and adhesion were used for comparison

between CTCs from CRPCa and castration sensitive prostate cancer (CSPCa) patients. The results suggest that CTCs from CRPCa were three times less stiff (more elastic), three times more deformable and seven times more adhesive than CSPCa CTCs. This established the relation between mechanical phenotypes as a novel biomarker for metastatic castration resistant prostate cancer [147]. A further investigation from the same authors revealed that interaction between CTCs and macrophages can increase the metastatic potential of CTCs by tuning their mechanical properties, which makes them fitter to survive the fluid shear stress imposed by blood circulation[148].

4.2 Biochemical Heterogeneity

4.2.1 Heterogeneous surface protein expression

As discussed earlier, tumor cells have numerous heterogeneities when it comes to protein expression and there have been numerous studies published with spiked tumor cell samples, which attempt to identify these heterogeneities using various microfluidic platforms as a proof of concept. However, profiling protein expressions and identifying heterogeneities is just one step towards unfolding the mystery of cancer heterogeneity. Correlating these protein expression profiles of patient CTCs with chemotherapeutic response is a highly desirable next step in the process. Here we will discuss some exploring effort on using clinical CTC samples to establish correlation between protein expression and chemotherapeutic response among cancer patients.

Green *et al.* used a microfluidic device with X-shaped posts to profile CTCs from patients with metastatic castrate resistant prostate cancer (mCRPCa). CTCs were tagged with IMNPs to differentiate cells into different zones based on EpCAM expression levels. Blood samples of 36 patients undergoing androgen depravation therapy (ADT) with either abiraterone or enzalutamide were collected and analyzed over the course of treatment (0 weeks to 9-22 weeks). This study

revealed lowering of EpCAM expression on CTCs during the course of treatment. This was reflected by higher numbers of CTCs captured in low-EpCAM zones of the microfluidic device, as compared to baseline numbers before therapy. As a comparison, the authors used CellSearch technique and but it was unable to capture the low-EpCAM CTCs [41]. This study demonstrated the effectiveness of using a microfluidic device in monitoring changes in the molecular profile of CTCs over a course of treatment.

Tayama *et al.* studied the impact of EpCAM expression on the effect of first line chemotherapeutic agent, cisplatin, and clinical outcome of the therapy in patients with epithelial ovarian cancer [149]. Their study demonstrated that ovarian cancer patients expressing high levels of EpCAM tend to have poor prognostic outcomes. Their subsequent study in mouse model also demonstrated that cisplatin tends to preferentially eliminate EpCAM-negative cells as compared to EpCAM-positive cells, and these positive cells contribute to further recurrences after chemotherapy. This study established a correlation between EpCAM expression levels and platinum-based chemotherapy in epithelial ovarian cancer.

Apart from EpCAM, which is the most explored antigen in research on CTCs, HER2 and estrogen receptor (ER) also have a significant impact on chemotherapeutic response in breast cancers. Presence of HER2-positive CTCs at various stages of breast cancer has been found to be an adverse prognostic factor for primary and metastatic breast cancer [150, 151]. A couple of studies demonstrated the efficacy of Trastuzumab, an anti-HER2 monoclonal antibody, in reducing the CTC count in HER2-negative primary breast cancer patients, indicating the presence of HER2-positive CTCs [151-153]. In another study, Maurizio Scaltriti and co-workers studied the effect of combination of two anti-HER2 chemotherapeutic agents, Lapatinib and Trastuzumab, in high HER2 expression cancer patients. Their study concluded that increasing HER2 expression has a

direct correlation to addition of Lapatinib to anti-HER2 therapy in combination with Trastuzumab, which was indicated by a higher pathological complete response and progression free survival of patients [154]. ER expression levels is also equally principal as HER2 expression to determine the target for hormonal therapy. However, studies exploring the clinical significance of ER expression are lacking to date [151].

In another recent study, Reza *et al.* used a SERS-based microfluidic platform for profiling three different melanoma associated surface proteins (melanoma-chondroitin sulfate proteoglycan (MCSP), melanoma cell adhesion molecule (MCAM), and low-affinity nerve growth factor receptor (LNGFR)) over the course of drug treatment with BRAF inhibitor PLX4720. The authors demonstrated the ability of PLX4720 to reduce heterogeneity in melanoma patients and identified subpopulations of CTCs maintained their protein expression even after the therapy, indicating therapeutic resistance [42]. Extent of cellular heterogeneity was correlated with overall survival rate and choice of therapy in metastatic CRPCa patients by Scher *et al.* They demonstrated that low CTC heterogeneity is connected to higher overall survival rate in patients treated with androgen receptor signaling inhibitor (ARSI), and high CTC heterogeneity is associated with higher overall survival rate in patients treated with Taxane chemotherapy [155]. This study showed that extent of heterogeneity among CTCs can help taking an informed decision regarding the choice of therapy.

Programmed death-ligand 1 (PD-L1) has also been identified as a crucial marker for prognostic applications [156]. PD-L1 is associated with poor clinical outcomes and is primarily overexpressed by the cells in head and neck carcinoma, melanoma, hepatocellular carcinoma, gastric cancer, ovarian cancer, bladder cancer, non-small cell lung cancer (NSCLC), etc. This protein is responsible for inhibition of T-cell mediated immune response [157]. A recent study from

Kowanetz *et al*. revealed that treating metastatic NSCLC patients expressing high PD-L1 with atezolizumab (anti-PD-L1 antibody), gave a robust response to the treatment. Thus, proving that lowering the expression of PD-L1 can have a positive impact on immune response [158].

In addition to these studies, correlations between E-cadherin, β-catenin and vimentin and diagnosis, prognosis and possible treatment resistance have also been established. Under expression of E-cadherin and β-catenin has been associated with advancement in cancer stages in naive prostate cancer and drug resistance to 5-Fluorouracil and Methotrexate in colorectal cancer [159, 160]. In addition, overexpression of Vimentin has been associated with treatment resistance to androgen deprivation therapy (ADT) with Abiraterone-acid and Taxanes and poor clinical outcome in acute myeloid leukemia patients[159, 161].

4.2.2 Chemotactic heterogeneity

High cellular motility driven by chemotaxis and biophysical properties of CTCs significantly promote metastatic events in cancer. Hence, it is of great importance to analyze single motile CTCs to better understand metastasis process and identify invasive phenotypes [162-164]. Due to rarity of CTCs in patient blood, most of the studies to date have been focused on chemotaxis of tumor cell lines instead of CTCs from patient blood. Here we will discuss some of the clinical studies on CTC migration and its impact on chemotherapeutic response.

Liu *et al.* in their recent study separated CTCs from patient blood using an integrated inertial ferrohydrodynamic cell separation (i^2FCS) method and then performed single cell migration assays for identifying functional phenotypes of isolated CTCs. Migration of single cells was tracked for 24h in confined channels with spatial concentration gradient of epidermal growth factor (EGF), basic fibroblast growth factor (bFGF) and FBS as chemoattractants. A total of 5000 micro tracks

30μm wide, 5μm high and 1200μm long, were fabricated for the assay. Cells were loaded and allowed to migrate towards the chemoattractant gradient for 24h as depicted in Figure 7C-(I) and (II). After 24h, cells were stained with fluorescent EpCAM, Vimentin, CD45 and DAPI, within the microchannel to identify surface expression. (Figure 7C-(III)). This method was able to profile chemotaxis and surface protein expression of CTCs in an integrated technique [115].

This study was continued by the same authors with the term CTC-Race assay to analyze chemotactic migration of CTCs from metastatic NSCLC patients followed by simultaneous biophysical and biochemical characterization at single cell resolution. CTCs from 4 NSCLC patients in late stage (stage IIIB-IV) were isolated using the similar i^2FCS method as earlier. These CTCs were then subjected to CTC-Race assay with the same chemoattractant gradient as the previous study. The assay revealed that CTCs of patient 1 migrated the most and at the fastest speed among the 4 patients at 0.26 ± 0.19 μm min^{-1}. Following the CTC-Race assay the cells were subjected to immunofluorescent assay with EpCAM and Vimentin which revealed high mesenchymal (Vimentin+) characteristics of CTCs from patient 1 as compared to CTCs from other 3 patients. Further, genetic characterization revealed that patient 1 exhibited highest tumor mutational burden (TMB) and PD-L1 expression which regulate the frequency of genetic mutations, and invasion and migration of cancer cells respectively [43].

Guo *et al.* studied the effect of CXCR2 inhibitor on myeloid cell chemotaxis and whether it could inhibit their resistance to ARSI. For this study, patients with metastatic CRPCa resistant to ARSI were treated with combination of CXCR2 and enzalutamide. The results indicated that the combination therapy was well tolerated by the patients with reduced intratumor myeloid infiltration due to reduced chemotaxis by CXCR2 inhibitor [165].

4.2.3 Metabolic heterogeneity

Metabolic heterogeneity in terms of MMP activity was demonstrated by integrated vortex capture and single cell droplet encapsulation mediated assay using samples of seven prostate cancer patients. As described previously, MMP activity was translated into fluorescence intensity of the droplet triggered by MMP-cleavable peptide substrate. Six of seven patients had CTCs and 87% of those CTCs showed MMP activity triggering fluorescence signals above baseline. The patient sample with no CTCs was found to have no new metastases. CTCs from patients which had lower levels of prostate specific antigen (PSA) expression showed a response to treatment and were found to have lower MMP secretion levels. While patients with radiographic progression to lymph node and bone marrow, revealed a higher number of CTCs secreting MMPs that is one order of magnitude higher than baseline levels of MMPs [128]. This study proved the clinical translation of this technique in identifying metabolic heterogeneity among different CTC phenotypes.

Metabolic changes in lung and ovarian cancer cells in response to Cisplatin treatments and resistance development have also been studied. Cancer cells develop resistance to cisplatin by alteration in their energy metabolism as compared to cisplatin sensitive cells. For example, glycolysis levels were found to be much higher in cisplatin-resistance ovarian cancer cells as compared to other sensitive cells. This phenomenon makes cisplatin resistant ovarian cancer cells sensitive to 2-deoxygluocose treatment due to glucose starvation mechanism. On the other hand, lung cancer cells rely on oxidative phosphorylation for energy and in turn have lower rates of glycolysis. This makes 2-deoxyglucose treatment less effective for cisplatin resistant lung cancer cells in normal conditions. But those cells are more sensitive to 2-deoxyglucose in hypoxic conditions, since cells have to depend on glycolysis for energy due to lack of oxygen for phosphorylation [166].

From these studies, it is clear that detection of metabolic heterogeneity among CTCs can reveal information regarding the aggressiveness of the disease, help clinicians determine the course of treatment and also help to manipulate metabolic properties in order to reduce chemotherapeutic resistance.

In addition to these clinically relevant studies, several efforts to standardize such assays are under way in Europe (the EU Innovative Medicines Initiative (IMI) consortium CANCER-ID or the European Liquid Biopsy Society (ELBS)) and the US (the Blood Profiling Atlas in Cancer (BloodPAC) consortium). There are also some ongoing clinical trials such as DETECT-IV in breast cancer, CABA-V7 in prostate cancer where therapeutic decisions are being made through CTC phenotypic characterization along with some ctDNA detection techniques such as TACT-D in metastatic colorectal cancer, c-TRACK-TN in the early stages of breast cancer [167].

Table 2. – List of cancer cell lines and clinical samples used for CTC phenotyping/profiling along with the method of microfluidic phenotyping and biomarkers targeted for profiling -

Ref	Cell Types	Cell origin	Mixture/single	Microfluidic phenotypic profiling/sorting method	Biomarker
62	HeLa cells (Treated with Latrunculin A and Paclitaxel)	Cervical	Single cell	Mechanical profiling	Deformability before and after treatment with different drugs
63	MCF-7, MCF-7 (treated with TPA), SKBR-3, MDA-MB-231, SUM149, SUM159	Breast	Single cell	Mechanical profiling	Transportability/elastic modulus/cell diameter
64	MCF-7 and MDA-MB-231	Breast	Single cell	Mechanical profiling	Cell–substrate adhesion/elastic modulus
	CL-1 and LnCaP	Prostate			
65	MCF-7	Breast	Single cell	Mechanical profiling	Deformability and EpCAM expression
	HeLa	Cervical			
	PC3	Prostate			
66	PC3, DU145, LnCaP	Prostate	Single cell	Mechanical profiling	Correlating androgen sensitivity and deformability
70	HT29, Caco2	Colon	Single cell	Mechanical profiling	Deformability/ALDH activity/stemness character
	HeLa	Cervical			
	MDA-MB-231	Breast			
	Jurkat	Peripheral blood			
71	SUM149 (ALDH+/ALDH-)	Breast	Single cell	Mechanical profiling	Deformability/adhesion under shear/ALDH activity
72	A549 (stem cells/non-stem cells)	Lung	Single cell	Mechanical profiling	Deformability/low or high adhesion/stemness
80	PC3, LnCaP, RWPE-1	Prostate	Single cell	Electrical profiling	Dielectrophoretic motion
81	MCF-7, MCF-7 (PMA modified)	Breast	Single cell	Electrical profiling	Electrical impedance/deformability

83	MCF-7, MDA-MB-231 and MDA-MB-468	Breast	Single cell	Electrical profiling	Dielectric polarizability
77	MCF-7 and MDA-MB-231	Breast	Single cell	Electrical profiling	Conductivity and permittivity
91	PANC-1 cell (inherent heterogeneity)	Pancreatic	Cell mixture	Surface antigen-based sorting with IMNP	EpCAM
92	VCaP	Prostate	Cell mixture	Surface antigen-based sorting with IMNP	EpCAM
	SK-BR-3 cells, MDA-MB-231 cells	Breast			
93	SKBR3, MDA-MB-231	Breast	Cell mixture	Surface antigen-based sorting with IMNP	EpCAM
94	MDA-MB-231, MCF-7, SKBR3, SKBR3 (CoCl2 treated)	Breast	Cell mixture	Surface antigen-based sorting with IMNP	EpCAM
95	MCF-7, SKBR3, MDA-MB-231	Breast	Cell mixture	Surface antigen-based sorting with IMNP	EpCAM
	PC3	Prostate			
96, 97, 98	MDA-MB-231, SKBR3	Breast	Cell mixture	Surface antigen-based sorting with IMNP	EpCAM
	VCaP	Prostate			
99	MDA-MB-231, MDA-ECAD (more epithelial due to E-cadherin)	Breast	Cell mixture	Surface antigen-based sorting with IMNP	Cluster size/EpCAM
100	MCF-7, MDA-MB-231, SK-BR-3	Breast	Cell mixture	Surface antigen-based sorting with IMNP	EpCAM
101	MDA-MB-231, SKBR3	Breast	Cell mixture	Surface antigen-based sorting with IMNP	EpCAM
	PC3	Prostate			
103	HeLa	Cervical	Single cell	Surface antigen-based sorting with IMNP	Folate receptor
	A549	Lung			
104	MDA-MB-231, SK-BR-3, and MCF-7	Breast	Cell mixture	Surface antigen-based sorting with IMNP	EpCAM
106	Kato III	Stomach	Cell mixture		EpCAM

	SW 480	Large intestine; Colon		Surface antigen-based sorting without IMNP	
	HuH-7	Liver			
107	HuH-7 and SK-HEP-1 cells	Liver	Cell mixture	Surface antigen-based sorting without IMNP	EpCAM, ASGPR
	HCC	Breast			
	CCRF-CEM	Peripheral blood			
103	MCF-7, MDA-MB-231	Breast	Cell mixture	Surface antigen-based sorting without IMNP	EpCAM, cocktail (Axl, PD-L1, EGFR)
117	SKOV3, A2780DK	Ovarian	Single cell	Chemotactic sorting	Chemoattractant: hepatocyte growth factor (HGF), fetal bovine serum
	PC3	Prostate			
	MDA-MB-231, MDA-MB-231(GKD)	Breast			
118	MCF7, SUM159	Breast	Single cell	Chemotactic sorting	Chemoattractant: FITC-labeled bovine serum albumin (BSA)
119	MDA-MB-231	Breast	Single cell	Chemotactic sorting	Chemoattractant: epidermal growth factor (EGF)
116	HT-29	Colorectal	Single cell	Chemotactic sorting	Chemoattractant: Fetal bovine serum (FBS)
	SGC-7901	Gastric			
	A549	Lung			
114	Lung Cancer Stem Cell (LCSC)	Lung	Single cell	Chemotactic sorting	Chemoattractant: Fetal bovine serum (FBS)
	Differentiated Lung Cancer Stem Cell (dLCSC)				
128	A549, HCC827	Lung	Single cell	Metabolic sorting	Enzyme: Matrix metalloproteases (MMPs)
	VCaP, LnCaP, PC3	Prostate			
127	MDA-MB-231	Breast	Cell mixture	Metabolic sorting	Glycolytic activity
	K-562	Bone marrow			
126	U87	Glioblastoma	Cell mixture	Metabolic sorting	Glycolytic activity
125	MCF7	Breast	Single cell	Metabolic sorting	Over 120 metabolites analyzed
	HepG2	Liver			

41	Patient samples	Prostate	Surface antigen-based sorting with IMNP	EpCAM
42	Patient samples	Melanoma	Surface antigen-based sorting with IMNP	MCSP, MCAM, LNGFR
115	Patient samples	Not specified	Chemotactic sorting	Chemoattractant: epidermal growth factor (EGF), basic fibroblast growth factor (bFGF), FBS
43	Patient samples	Lung	Chemotactic sorting	Chemoattractant: epidermal growth factor (EGF), basic fibroblast growth factor (bFGF), FBS
44	Mouse xenograft	Lung	Mechanical profiling	Deformability/low or high adhesion/stemness
128	Patient samples	Prostate	Metabolic sorting	Enzyme: Matrix metalloproteases (MMPs)

5 Outlook

After going through the existing studies on CTC profiling methods, making further advances in this field appears to be a necessity for rapid processing of clinically relevant samples. Considering the low frequency of CTCs in blood, building integrated platforms for high efficiency isolation and in-situ profiling of biomarkers would prove to be effective in rapid cancer prognosis, diagnosis and treatment monitoring.

CTC profiling methods which would establish a multi-dimensional relation between surface antigen expression, metabolism, chemotaxis, gene expression, mechanical and electrical characteristics and stemness markers with metastatic potential, survival rate and drug response are essential. Some techniques currently used for mechanical phenotyping seem to be much less practical in clinical settings as compared to microfluidic approaches, considering necessity of high throughput, low cost and compatibility with low frequency of CTCs in blood samples. Since expression of different surface antigens is one of the most important indicators of metastatic potential of CTCs, integrated profiling of EpCAM, HER2, EGFR, PD-L1 and many such antigens of captured CTCs in a single platform would prove to be instrumental in understanding the molecular nature of the disease. There are very few studies on CTC surface antigen profiling by non-magnetic microfluidic approaches available in literature. New methods of microfluidic biomarker profiling without tagging cells with IMNPs are necessary to eliminate cell stress for viability and phenotype preservation. Development of microfluidic platforms with *in-situ* sequencing ability for ctDNA and cfRNA analysis along with conventional CTC profiling and phenotyping would be a significant addition for cancer diagnostics.

According to recent statistics of cancer diagnosis, breast, lung and prostate cancers are the most commonly diagnosed cancers worldwide [168]. From Table 2, breast and prostate cancer cell lines are used in most of the in-vitro studies. Lung cancer cell lines seem to be under explored in this field. More studies with various lung cancer cell lines are necessary for better understanding of the nature of this second most commonly diagnosed cancer type. In addition, significant efforts are required to identify responses of different CTC phenotypes to various anti-cancer drugs. This would help in identifying drug resistant phenotypes for development of highly efficient drug combination therapies. In order to achieve this objective, development of drug screening platforms which could capture the changes in biophysical and biochemical characteristics before and after drug treatment are necessary. These platforms will guide clinicians in the development of personalized therapies based on the molecular profile of individual patients and treatment monitoring. Moreover, prediction of the mechanisms of action of drugs may be done by monitoring changes in biomarkers on CTCs captured from blood samples.

Acronyms

CTCs – Circulating Tumor Cells

EpCAM – Epithelial Cell Adhesion Molecule

EMT – Epithelial to Mesenchymal Transition

MET – Mesenchymal to Epithelial Transition

CSCs – Cancer Stem Cells

FACS - Fluorescence Activated Cell Sorting

ALDH – Aldehyde Dehydrogenase

IBC – Inflammatory Breast Cancer

MS-chip – Mechanical Sorting Chip

HCA-chip – High Throughput Adhesion Chip

DEP – Dielectrophoresis

Re[CMF] – Clausius-Mossotti Factor

MNU – N-methyl-N-nitrosourea

PMA – 12-myristate-13-acetate

modMCF7 – modified MCF7

CPF – Characteristic Polarizability Frequency

HER2 – Human Epidermal Growth Factor Receptor 2

EGFR – Epidermal Growth Factor Receptor

ASGPR - Asialoglycoprotein Receptor

PSMA – Prostate Specific Membrane Antigen

FiSH – Fluorescence *in-situ* Hybridization

IMNP – Immunomagnetic Nanoparticles

NIR – Near Infrared

LFM – Lateral Flow Microarray

SDI – Size Dictated Immunocapture

DLD – Deterministic Lateral Displacement

HCC – Hepatocellular Carcinoma

LCSCs – Lung Cancer Stem Cells

dLSCSs – Differentiated Lung Cancer Stem Cells

NADPH - Nicotinamide Adenine Dinucleotide Phosphate

PEF-ESI-HRMS - Pulsed Electric Field-Induced Electrospray Ionization-High Resolution Mass Spectrometry

SIFT – Sorting by Interfacial Tension

2DG – 2-deoxy-D-glucose

MMPs – Matrix Metalloproteases

ECM – Extracellular Matrix

qRT-PCR – Quantitative Real Time Reverse Transcription

ctDNA – Circulating Tumor DNA

cfRNA – Cell Free miRNA

EVs – Extracellular Vesicles

ISL – A Natural Flavonoid Derived from Licorice

CRPCa – Castration Resistant Prostate Cancer

CSPCa – Castration Sensitive Prostate Cancer

ADT – Androgen Depravation Therapy

ER – Estrogen Receptor

MCSP - Melanoma-Chondroitin Sulfate Proteoglycan

MCAM - Melanoma Cell Adhesion Molecule

LNGFR - Low-Affinity Nerve Growth Factor Receptor

ARSI - Androgen Receptor Signaling Inhibitor

NSCLC – Non-Small Cell Lung Cancer

PD-L1 - Programmed Death Ligand

i^2FCS - Integrated Inertial Ferrohydrodynamic Cell Separation

EGF - Epidermal Growth Factor

bFGF - Basic Fibroblast Growth Factor

TMB – Tumor Mutation Burden

Conflict of Interest

Authors declare no conflicts of interest.

Author Contributions

RJ: Conceptualization, data curation, writing-original draft, writing-review and editing. HA: Writing-original draft, writing-review and editing. KG: Writing-original draft, writing-review and editing. RKB: Writing-original draft, writing-review and editing. WW: Writing-original draft, writing-review and editing. WL: Conceptualization, writing–original draft, writing–review and editing, supervision.

Acknowledgements

WL acknowledges support from National Science Foundation (CBET, Grant No. 1935792) and National Institute of Health (IMAT, Grant No. 1R21CA240185-01).

References

[1] H. Wang, M. Naghavi, C. Allen, R.M. Barber, Z.A. Bhutta, A. Carter, D.C. Casey, F.J. Charlson, A.Z. Chen, M.M. Coates, Global, regional, and national life expectancy, all-cause mortality, and cause-specific mortality for 249 causes of death, 1980–2015: a systematic analysis for the Global Burden of Disease Study 2015, The lancet, 388 (2016) 1459-1544.
[2] C.L. Chaffer, R.A. Weinberg, A perspective on cancer cell metastasis, science, 331 (2011) 1559-1564.
[3] E.C. Woodhouse, R.F. Chuaqui, L.A. Liotta, General mechanisms of metastasis, Cancer: Interdisciplinary International Journal of the American Cancer Society, 80 (1997) 1529-1537.
[4] M.-Y. Kim, T. Oskarsson, S. Acharyya, D.X. Nguyen, X.H.-F. Zhang, L. Norton, J. Massagué, Tumor self-seeding by circulating cancer cells, Cell, 139 (2009) 1315-1326.
[5] M. Tellez-Gabriel, M.-F. Heymann, D. Heymann, Circulating tumor cells as a tool for assessing tumor heterogeneity, Theranostics, 9 (2019) 4580.
[6] S. Mocellin, D. Hoon, A. Ambrosi, D. Nitti, C.R. Rossi, The prognostic value of circulating tumor cells in patients with melanoma: a systematic review and meta-analysis, Clinical cancer research, 12 (2006) 4605-4613.
[7] R.T. Krivacic, A. Ladanyi, D.N. Curry, H. Hsieh, P. Kuhn, D.E. Bergsrud, J.F. Kepros, T. Barbera, M.Y. Ho, L.B. Chen, A rare-cell detector for cancer, Proceedings of the National Academy of Sciences, 101 (2004) 10501-10504.
[8] R. Rosenberg, R. Gertler, J. Friederichs, K. Fuehrer, M. Dahm, R. Phelps, S. Thorban, H. Nekarda, J. Siewert, Comparison of two density gradient centrifugation systems for the enrichment of disseminated tumor cells in blood, Cytometry: The Journal of the International Society for Analytical Cytology, 49 (2002) 150-158.

[9] S. Khetani, M. Mohammadi, A.S. Nezhad, Filter‐based isolation, enrichment, and characterization of circulating tumor cells, Biotechnology and bioengineering, 115 (2018) 2504-2529.
[10] B. Kwak, S. Lee, J. Lee, J. Lee, J. Cho, H. Woo, Y.S. Heo, Hydrodynamic blood cell separation using fishbone shaped microchannel for circulating tumor cells enrichment, Sensors and Actuators B: Chemical, 261 (2018) 38-43.
[11] H.-S. Moon, K. Kwon, K.-A. Hyun, T. Seok Sim, J. Chan Park, J.-G. Lee, H.-I. Jung, Continual collection and re-separation of circulating tumor cells from blood using multi-stage multi-orifice flow fractionation, Biomicrofluidics, 7 (2013) 014105.
[12] P.R. Gascoyne, S. Shim, Isolation of circulating tumor cells by dielectrophoresis, Cancers, 6 (2014) 545-579.
[13] S. Riethdorf, H. Fritsche, V. Müller, T. Rau, C. Schindlbeck, B. Rack, W. Janni, C. Coith, K. Beck, F. Jänicke, Detection of circulating tumor cells in peripheral blood of patients with metastatic breast cancer: a validation study of the CellSearch system, Clinical cancer research, 13 (2007) 920-928.
[14] F. Nolé, E. Munzone, L. Zorzino, I. Minchella, M. Salvatici, E. Botteri, M. Medici, E. Verri, L. Adamoli, N. Rotmensz, Variation of circulating tumor cell levels during treatment of metastatic breast cancer: prognostic and therapeutic implications, Annals of Oncology, 19 (2008) 891-897.
[15] D.L. Adams, R.K. Alpaugh, S. Tsai, C.-M. Tang, S. Stefansson, Multi-Phenotypic subtyping of circulating tumor cells using sequential fluorescent quenching and restaining, Scientific reports, 6 (2016) 1-9.
[16] B. Vogelstein, N. Papadopoulos, V.E. Velculescu, S. Zhou, L.A. Diaz Jr, K.W. Kinzler, Cancer genome landscapes, science, 339 (2013) 1546-1558.
[17] E. Kilgour, D.G. Rothwell, G. Brady, C. Dive, Liquid biopsy-based biomarkers of treatment response and resistance, Cancer cell, 37 (2020) 485-495.
[18] M. López-Lázaro, The stem cell division theory of cancer, Critical Reviews in Oncology/Hematology, 123 (2018) 95-113.
[19] J. Massagué, A.C. Obenauf, Metastatic colonization by circulating tumour cells, Nature, 529 (2016) 298-306.
[20] B. Strilic, S. Offermanns, Intravascular survival and extravasation of tumor cells, Cancer cell, 32 (2017) 282-293.
[21] A. Marusyk, V. Almendro, K. Polyak, Intra-tumour heterogeneity: a looking glass for cancer?, Nature reviews cancer, 12 (2012) 323-334.
[22] T. Tsuji, S. Ibaragi, G.-f. Hu, Epithelial-mesenchymal transition and cell cooperativity in metastasis, Cancer research, 69 (2009) 7135-7139.
[23] F. Liu, L.N. Gu, B.E. Shan, C.Z. Geng, M.X. Sang, Biomarkers for EMT and MET in breast cancer: An update, Oncology letters, 12 (2016) 4869-4876.
[24] J. Roche, The epithelial-to-mesenchymal transition in cancer, MDPI, 2018, pp. 52.
[25] K. Gravdal, O.J. Halvorsen, S.A. Haukaas, L.A. Akslen, A switch from E-cadherin to N-cadherin expression indicates epithelial to mesenchymal transition and is of strong and independent importance for the progress of prostate cancer, Clinical cancer research, 13 (2007) 7003-7011.
[26] D. Yao, C. Dai, S. Peng, Mechanism of the mesenchymal–epithelial transition and its relationship with metastatic tumor formation, Molecular cancer research, 9 (2011) 1608-1620.
[27] M. Poudineh, E.H. Sargent, K. Pantel, S.O. Kelley, Profiling circulating tumour cells and other biomarkers of invasive cancers, Nature Biomedical Engineering, 2 (2018) 72-84.
[28] M. Labib, S.O. Kelley, Circulating tumor cell profiling for precision oncology, Molecular oncology, 15 (2021) 1622-1646.
[29] H. Esmaeilsabzali, T.V. Beischlag, M.E. Cox, A.M. Parameswaran, E.J. Park, Detection and isolation of circulating tumor cells: Principles and methods, Biotechnology Advances, 31 (2013) 1063-1084.

[30] L. Wu, X. Xu, B. Sharma, W. Wang, X. Qu, L. Zhu, H. Zhang, Y. Song, C. Yang, Beyond capture: circulating tumor cell release and single‐cell analysis, Small Methods, 3 (2019) 1800544.
[31] Y. Liu, R. Li, L. Zhang, S. Guo, Nanomaterial-based immunocapture platforms for the recognition, isolation, and detection of circulating tumor cells, Frontiers in bioengineering and biotechnology, 10 (2022) 850241.
[32] L. Wu, L. Zhu, M. Huang, J. Song, H. Zhang, Y. Song, W. Wang, C. Yang, Aptamer-based microfluidics for isolation, release and analysis of circulating tumor cells, TrAC Trends in Analytical Chemistry, 117 (2019) 69-77.
[33] Q. Shen, L. Xu, L. Zhao, D. Wu, Y. Fan, Y. Zhou, W.H. OuYang, X. Xu, Z. Zhang, M. Song, Specific capture and release of circulating tumor cells using aptamer‐modified nanosubstrates, Advanced materials, 25 (2013) 2368-2373.
[34] Y. Huang, X. Li, J. Hou, Z. Luo, G. Yang, S. Zhou, Conductive Nanofibers-Enhanced Microfluidic Device for the Efficient Capture and Electrical Stimulation-Triggered Rapid Release of Circulating Tumor Cells, Biosensors, 13 (2023) 497.
[35] K.H. Neoh, S.K.S. Cheng, H. Wu, A. Chen, Y. Sun, B. Li, A. Cao, R.P. Han, pH-responsive carbon nanotube film-based microfluidic chip for efficient capture and release of cancer cells, ACS Applied Nano Materials, 5 (2022) 6911-6924.
[36] M.-H. Park, E. Reátegui, W. Li, S.N. Tessier, K.H. Wong, A.E. Jensen, V. Thapar, D. Ting, M. Toner, S.L. Stott, Enhanced isolation and release of circulating tumor cells using nanoparticle binding and ligand exchange in a microfluidic chip, Journal of the American Chemical Society, 139 (2017) 2741-2749.
[37] W. Li, E. Reátegui, M.-H. Park, S. Castleberry, J.Z. Deng, B. Hsu, S. Mayner, A.E. Jensen, L.V. Sequist, S. Maheswaran, Biodegradable nano-films for capture and non-invasive release of circulating tumor cells, Biomaterials, 65 (2015) 93-102.
[38] E. Reátegui, N. Aceto, E.J. Lim, J.P. Sullivan, A.E. Jensen, M. Zeinali, J.M. Martel, A.J. Aranyosi, W. Li, S. Castleberry, Tunable nanostructured coating for the capture and selective release of viable circulating tumor cells, Advanced Materials (Deerfield Beach, Fla.), 27 (2015) 1593.
[39] D. Yu, L. Tang, Z. Dong, K.A. Loftis, Z. Ding, J. Cheng, B. Qin, J. Yan, W. Li, Effective reduction of non-specific binding of blood cells in a microfluidic chip for isolation of rare cancer cells, Biomaterials science, 6 (2018) 2871-2880.
[40] H.K. Brown, M. Tellez-Gabriel, P.-F. Cartron, F.M. Vallette, M.-F. Heymann, D. Heymann, Characterization of circulating tumor cells as a reflection of the tumor heterogeneity: myth or reality?, Drug Discovery Today, 24 (2019) 763-772.
[41] B.J. Green, V. Nguyen, E. Atenafu, P. Weeber, B.T. Duong, P. Thiagalingam, M. Labib, R.M. Mohamadi, A.R. Hansen, A.M. Joshua, Phenotypic profiling of circulating tumor cells in metastatic prostate cancer patients using nanoparticle-mediated ranking, Analytical chemistry, 91 (2019) 9348-9355.
[42] K.K. Reza, S. Dey, A. Wuethrich, J. Wang, A. Behren, F. Antaw, Y. Wang, A.A.I. Sina, M. Trau, In situ single cell proteomics reveals circulating tumor cell heterogeneity during treatment, ACS nano, 15 (2021) 11231-11243.
[43] Y. Liu, W. Zhao, J. Hodgson, M. Egan, C.N. Cooper Pope, G. Hicks, P.G. Nikolinakos, L. Mao, CTC-Race: Single-Cell Motility Assay of Circulating Tumor Cells from Metastatic Lung Cancer Patients, ACS nano, 18 (2024) 8683-8693.
[44] Y. Jia, P. Shen, T. Yan, W. Zhou, J. Sun, X. Han, Microfluidic tandem mechanical sorting system for enhanced cancer stem cell isolation and ingredient screening, Advanced Healthcare Materials, 10 (2021) 2100985.
[45] P.R. Srinivas, B.S. Kramer, S. Srivastava, Trends in biomarker research for cancer detection, The Lancet Oncology, 2 (2001) 698-704.

[46] E. Jonietz, The forces of cancer, Nature, 491 (2012) S56-S57.
[47] A. Salmanzadeh, M.B. Sano, R.C. Gallo-Villanueva, P.C. Roberts, E.M. Schmelz, R.V. Davalos, Investigating dielectric properties of different stages of syngeneic murine ovarian cancer cells, Biomicrofluidics, 7 (2013) 011809.
[48] M. Yang, W.J. Brackenbury, Membrane potential and cancer progression, Frontiers in physiology, 4 (2013) 185.
[49] P.Y. Liu, L. Chin, W. Ser, H. Chen, C.-M. Hsieh, C.-H. Lee, K.-B. Sung, T. Ayi, P. Yap, B. Liedberg, Cell refractive index for cell biology and disease diagnosis: past, present and future, Lab on a Chip, 16 (2016) 634-644.
[50] V. Backman, M.B. Wallace, L. Perelman, J. Arendt, R. Gurjar, M. Müller, Q. Zhang, G. Zonios, E. Kline, T. McGillican, Detection of preinvasive cancer cells, Nature, 406 (2000) 35-36.
[51] Y. Shen, B.U.S. Schmidt, H. Kubitschke, E.W. Morawetz, B. Wolf, J.A. Käs, W. Losert, Detecting heterogeneity in and between breast cancer cell lines, Cancer Convergence, 4 (2020) 1.
[52] A. Fuhrmann, A. Banisadr, P. Beri, T.D. Tlsty, A.J. Engler, Metastatic State of Cancer Cells May Be Indicated by Adhesion Strength, Biophysical Journal, 112 (2017) 736-745.
[53] M. Plodinec, M. Loparic, C.A. Monnier, E.C. Obermann, R. Zanetti-Dallenbach, P. Oertle, J.T. Hyotyla, U. Aebi, M. Bentires-Alj, R.Y.H. Lim, C.-A. Schoenenberger, The nanomechanical signature of breast cancer, Nature Nanotechnology, 7 (2012) 757-765.
[54] V. Swaminathan, K. Mythreye, E.T. O'Brien, A. Berchuck, G.C. Blobe, R. Superfine, Mechanical stiffness grades metastatic potential in patient tumor cells and in cancer cell linesmechanical stiffness of cells dictates cancer cell invasion, Cancer research, 71 (2011) 5075-5080.
[55] Y.M. Efremov, A.X. Cartagena-Rivera, A.I. Athamneh, D.M. Suter, A. Raman, Mapping heterogeneity of cellular mechanics by multi-harmonic atomic force microscopy, Nature Protocols, 13 (2018) 2200-2216.
[56] Z. Liu, S.J. Lee, S. Park, K. Konstantopoulos, K. Glunde, Y. Chen, I. Barman, Cancer cells display increased migration and deformability in pace with metastatic progression, The FASEB Journal, 34 (2020) 9307-9315.
[57] H. Pu, N. Liu, J. Yu, Y. Yang, Y. Sun, Y. Peng, S. Xie, J. Luo, L. Dong, H. Chen, Micropipette aspiration of single cells for both mechanical and electrical characterization, IEEE Transactions on Biomedical Engineering, 66 (2019) 3185-3191.
[58] S.M. Ahmmed, S.S. Bithi, A.A. Pore, N. Mubtasim, C. Schuster, L.S. Gollahon, S.A. Vanapalli, Multi-sample deformability cytometry of cancer cells, APL bioengineering, 2 (2018) 032002.
[59] P.B. van Wachem, T. Beugeling, J. Feijen, A. Bantjes, J.P. Detmers, W.G. van Aken, Interaction of cultured human endothelial cells with polymeric surfaces of different wettabilities, Biomaterials, 6 (1985) 403-408.
[60] F. Lautenschläger, S. Paschke, S. Schinkinger, A. Bruel, M. Beil, J. Guck, The regulatory role of cell mechanics for migration of differentiating myeloid cells, Proceedings of the National Academy of Sciences, 106 (2009) 15696-15701.
[61] L. Beunk, G.-J. Bakker, D. van Ens, J. Bugter, F. Gal, M. Svoren, P. Friedl, K. Wolf, Actomyosin contractility requirements and reciprocal cell–tissue mechanics for cancer cell invasion through collagen-based channels, The European Physical Journal E, 45 (2022) 48.
[62] M. Sano, N. Kaji, A.C. Rowat, H. Yasaki, L. Shao, H. Odaka, T. Yasui, T. Higashiyama, Y. Baba, Microfluidic mechanotyping of a single cell with two consecutive constrictions of different sizes and an electrical detection system, Analytical chemistry, 91 (2019) 12890-12899.
[63] Z. Liu, Y. Lee, Y. Li, X. Han, K. Yokoi, M. Ferrari, L. Zhou, L. Qin, Microfluidic cytometric analysis of cancer cell transportability and invasiveness, Scientific reports, 5 (2015) 1-12.
[64] S. Park, Y.J. Lee, AFM-based dual nano-mechanical phenotypes for cancer metastasis, Journal of biological physics, 40 (2014) 413-419.

[65] S. Hu, G. Liu, W. Chen, X. Li, W. Lu, R.H. Lam, J. Fu, Multiparametric biomechanical and biochemical phenotypic profiling of single cancer cells using an elasticity microcytometer, small, 12 (2016) 2300-2311.
[66] N. Liu, P. Du, X. Xiao, Y. Liu, Y. Peng, C. Yang, T. Yue, Microfluidic-based mechanical phenotyping of androgen-sensitive and non-sensitive prostate cancer cells lines, Micromachines, 10 (2019) 602.
[67] Z. Yu, T.G. Pestell, M.P. Lisanti, R.G. Pestell, Cancer stem cells, The International Journal of Biochemistry & Cell Biology, 44 (2012) 2144-2151.
[68] J. Lv, Y. Liu, F. Cheng, J. Li, Y. Zhou, T. Zhang, N. Zhou, C. Li, Z. Wang, L. Ma, Cell softness regulates tumorigenicity and stemness of cancer cells, The EMBO journal, 40 (2021) e106123.
[69] L.F. Kadem, K.G. Suana, M. Holz, W. Wang, H. Westerhaus, R. Herges, C. Selhuber‐Unkel, High‐Frequency Mechanostimulation of Cell Adhesion, Angewandte Chemie, 129 (2017) 231-235.
[70] M. Terada, S. Ide, T. Naito, N. Kimura, M. Matsusaki, N. Kaji, Label-Free Cancer Stem-like Cell Assay Conducted at a Single Cell Level Using Microfluidic Mechanotyping Devices, Analytical Chemistry, 93 (2021) 14409-14416.
[71] W. Chen, S.G. Allen, W. Qian, Z. Peng, S. Han, X. Li, Y. Sun, C. Fournier, L. Bao, R.H. Lam, Biophysical Phenotyping and Modulation of ALDH+ Inflammatory Breast Cancer Stem‐Like Cells, Small, 15 (2019) 1802891.
[72] P.R. Gascoyne, S. Shim, J. Noshari, F.F. Becker, K. Stemke‐Hale, Correlations between the dielectric properties and exterior morphology of cells revealed by dielectrophoretic field‐flow fractionation, Electrophoresis, 34 (2013) 1042-1050.
[73] J. Nourse, J. Prieto, A. Dickson, J. Lu, M. Pathak, F. Tombola, M. Demetriou, A. Lee, L.A. Flanagan, Membrane biophysics define neuron and astrocyte progenitors in the neural lineage, Stem Cells, 32 (2014) 706-716.
[74] I. Turcan, M.A. Olariu, Dielectrophoretic Manipulation of Cancer Cells and Their Electrical Characterization, ACS Combinatorial Science, 22 (2020) 554-578.
[75] C. Chung, M. Waterfall, S. Pells, A. Menachery, S. Smith, R. Pethig, Dielectrophoretic characterisation of mammalian cells above 100 MHz, Journal of Electrical Bioimpedance, 2 (2011) 64-71.
[76] C. Vaillier, T. Honegger, F. Kermarrec, X. Gidrol, D. Peyrade, Label-free electric monitoring of human cancer cells as a potential diagnostic tool, Analytical chemistry, 88 (2016) 9022-9028.
[77] Y. Wang, Y. Li, J. Huang, Y. Zhang, R. Ma, S. Zhang, T. Yin, S. Liu, Y. Song, Z. Liu, Correlation between electrical characteristics and biomarkers in breast cancer cells, Scientific Reports, 11 (2021) 14294.
[78] K. Heileman, J. Daoud, M. Tabrizian, Dielectric spectroscopy as a viable biosensing tool for cell and tissue characterization and analysis, Biosensors and Bioelectronics, 49 (2013) 348-359.
[79] G.I. Russo, N. Musso, A. Romano, G. Caruso, S. Petralia, L. Lanzanò, G. Broggi, M. Camarda, The Role of Dielectrophoresis for Cancer Diagnosis and Prognosis, Cancers, 14 (2022) 198.
[80] C. Vaillier, T. Honegger, F. Kermarrec, X. Gidrol, D. Peyrade, Comprehensive analysis of human cells motion under an irrotational AC electric field in an electro-microfluidic chip, PloS one, 9 (2014) e95231.
[81] Y. Zhou, D. Yang, Y. Zhou, B.L. Khoo, J. Han, Y. Ai, Characterizing deformability and electrical impedance of cancer cells in a microfluidic device, Analytical chemistry, 90 (2018) 912-919.
[82] I. Emerit, P.A. Cerutti, Tumour promoter phorbol-12-myristate-13-acetate induces chromosomal damage via indirect action, Nature, 293 (1981) 144-146.

[83] M. Jahangiri, M. Ranjbar-Torkamani, H. Abadijoo, M. Ghaderinia, H. Ghafari, A. Mamdouh, M. Abdolahad, Low frequency stimulation induces polarization-based capturing of normal, cancerous and white blood cells: a new separation method for circulating tumor cell enrichment or phenotypic cell sorting, Analyst, 145 (2020) 7636-7645.
[84] P.T. Went, A. Lugli, S. Meier, M. Bundi, M. Mirlacher, G. Sauter, S. Dirnhofer, Frequent EpCam protein expression in human carcinomas, Human pathology, 35 (2004) 122-128.
[85] J.B. Haun, C.M. Castro, R. Wang, V.M. Peterson, B.S. Marinelli, H. Lee, R. Weissleder, Micro-NMR for rapid molecular analysis of human tumor samples, Science translational medicine, 3 (2011) 71ra16-71ra16.
[86] J.B. Haun, N.K. Devaraj, S.A. Hilderbrand, H. Lee, R. Weissleder, Bioorthogonal chemistry amplifies nanoparticle binding and enhances the sensitivity of cell detection, Nature Nanotechnology, 5 (2010) 660-665.
[87] D.R. Glenn, K. Lee, H. Park, R. Weissleder, A. Yacoby, M.D. Lukin, H. Lee, R.L. Walsworth, C.B. Connolly, Single-cell magnetic imaging using a quantum diamond microscope, Nature methods, 12 (2015) 736-738.
[88] L. McInroy, A. Määttä, Down-regulation of vimentin expression inhibits carcinoma cell migration and adhesion, Biochemical and biophysical research communications, 360 (2007) 109-114.
[89] G. Agiostratidou, J. Hulit, G.R. Phillips, R.B. Hazan, Differential Cadherin Expression: Potential Markers for Epithelial to Mesenchymal Transformation During Tumor Progression, Journal of Mammary Gland Biology and Neoplasia, 12 (2007) 127-133.
[90] M. Santoni, M. Scarpelli, R. Mazzucchelli, A. Lopez-Beltran, L. Cheng, S. Cascinu, R. Montironi, Targeting prostate-specific membrane antigen for personalized therapies in prostate cancer: morphologic and molecular backgrounds and future promises, Journal of biological regulators and homeostatic agents, 28 (2014) 555-563.
[91] R. Jack, K. Hussain, D. Rodrigues, M. Zeinali, E. Azizi, M. Wicha, D.M. Simeone, S. Nagrath, Microfluidic continuum sorting of sub-populations of tumor cells via surface antibody expression levels, Lab on a Chip, 17 (2017) 1349-1358.
[92] J.D. Besant, R.M. Mohamadi, P.M. Aldridge, Y. Li, E.H. Sargent, S.O. Kelley, Velocity valleys enable efficient capture and spatial sorting of nanoparticle-bound cancer cells, Nanoscale, 7 (2015) 6278-6285.
[93] N. Muhanna, A. Mepham, R.M. Mohamadi, H. Chan, T. Khan, M. Akens, J.D. Besant, J. Irish, S.O. Kelley, Nanoparticle-based sorting of circulating tumor cells by epithelial antigen expression during disease progression in an animal model, Nanomedicine: Nanotechnology, Biology and Medicine, 11 (2015) 1613-1620.
[94] B.J. Green, L. Kermanshah, M. Labib, S.U. Ahmed, P.N. Silva, L. Mahmoudian, I.H. Chang, R.M. Mohamadi, J.V. Rocheleau, S.O. Kelley, Isolation of Phenotypically Distinct Cancer Cells Using Nanoparticle-Mediated Sorting, ACS Applied Materials & Interfaces, 9 (2017) 20435-20443.
[95] M. Poudineh, P.M. Aldridge, S. Ahmed, B.J. Green, L. Kermanshah, V. Nguyen, C. Tu, R.M. Mohamadi, R.K. Nam, A. Hansen, S.S. Sridhar, A. Finelli, N.E. Fleshner, A.M. Joshua, E.H. Sargent, S.O. Kelley, Tracking the dynamics of circulating tumour cell phenotypes using nanoparticle-mediated magnetic ranking, Nature Nanotechnology, 12 (2017) 274-281.
[96] R.M. Mohamadi, J.D. Besant, A. Mepham, B. Green, L. Mahmoudian, T. Gibbs, I. Ivanov, A. Malvea, J. Stojcic, A.L. Allan, Nanoparticle‐mediated binning and profiling of heterogeneous circulating tumor cell subpopulations, Angewandte Chemie International Edition, 54 (2015) 139-143.
[97] M. Poudineh, E.H. Sargent, S.O. Kelley, Amplified micromagnetic field gradients enable high-resolution profiling of rare cell subpopulations, ACS Applied Materials & Interfaces, 9 (2017) 25683-25690.

[98] M. Labib, B. Green, R.M. Mohamadi, A. Mepham, S.U. Ahmed, L. Mahmoudian, I.-H. Chang, E.H. Sargent, S.O. Kelley, Aptamer and antisense-mediated two-dimensional isolation of specific cancer cell subpopulations, Journal of the American Chemical Society, 138 (2016) 2476-2479.
[99] B.J. Green, M. Marazzini, B. Hershey, A. Fardin, Q. Li, Z. Wang, G. Giangreco, F. Pisati, S. Marchesi, A. Disanza, PillarX: A Microfluidic Device to Profile Circulating Tumor Cell Clusters Based on Geometry, Deformability, and Epithelial State, Small, 18 (2022) 2106097.
[100] O. Civelekoglu, N. Wang, M. Boya, T. Ozkaya-Ahmadov, R. Liu, A.F. Sarioglu, Electronic profiling of membrane antigen expression via immunomagnetic cell manipulation, Lab on a Chip, 19 (2019) 2444-2455.
[101] P.S. Williams, L.R. Moore, P. Joshi, M. Goodin, M. Zborowski, A. Fleischman, Microfluidic chip for graduated magnetic separation of circulating tumor cells by their epithelial cell adhesion molecule expression and magnetic nanoparticle binding, Journal of Chromatography A, 1637 (2021) 461823.
[102] E. Ozkumur, A.M. Shah, J.C. Ciciliano, B.L. Emmink, D.T. Miyamoto, E. Brachtel, M. Yu, P.-i. Chen, B. Morgan, J. Trautwein, A. Kimura, S. Sengupta, S.L. Stott, N.M. Karabacak, T.A. Barber, J.R. Walsh, K. Smith, P.S. Spuhler, J.P. Sullivan, R.J. Lee, D.T. Ting, X. Luo, A.T. Shaw, A. Bardia, L.V. Sequist, D.N. Louis, S. Maheswaran, R. Kapur, D.A. Haber, M. Toner, Inertial Focusing for Tumor Antigen–Dependent and –Independent Sorting of Rare Circulating Tumor Cells, Science Translational Medicine, 5 (2013) 179ra147-179ra147.
[103] C. Zhang, J. Lin, Y. Yu, D. Deng, Y. Yu, D. Zhang, Q. Zhong, Microfluidic Continuous Modification of Magnetic Nanoparticles for Circulating Tumor Cell Capture and Isolation, Advanced Materials Technologies, (2023) 2300062.
[104] S. Lv, D. Zheng, Z. Chen, B. Jia, P. Zhang, J. Yan, W. Jiang, X. Zhao, J.-J. Xu, Near-Infrared Light-Responsive Size-Selective Lateral Flow Chip for Single-Cell Manipulation of Circulating Tumor Cells, Analytical Chemistry, 95 (2022) 1201-1209.
[105] S.E. Gratton, P.A. Ropp, P.D. Pohlhaus, J.C. Luft, V.J. Madden, M.E. Napier, J.M. DeSimone, The effect of particle design on cellular internalization pathways, Proceedings of the national academy of sciences, 105 (2008) 11613-11618.
[106] M.G. Ahmed, M.F. Abate, Y. Song, Z. Zhu, F. Yan, Y. Xu, X. Wang, Q. Li, C. Yang, Isolation, Detection, and Antigen‐Based Profiling of Circulating Tumor Cells Using a Size‐Dictated Immunocapture Chip, Angewandte Chemie International Edition, 56 (2017) 10681-10685.
[107] L. Zhu, H. Lin, S. Wan, X. Chen, L. Wu, Z. Zhu, Y. Song, B. Hu, C. Yang, Efficient isolation and phenotypic profiling of circulating hepatocellular carcinoma cells via a combinatorial-antibody-functionalized microfluidic synergetic-chip, Analytical Chemistry, 92 (2020) 15229-15235.
[108] X. Wang, L. Deng, B.T. Gjertsen, A microfluidic device for differential capture of heterogeneous rare tumor cells with epithelial and mesenchymal phenotypes, Analytica Chimica Acta, 1129 (2020) 1-11.
[109] P. Gassmann, A. Enns, J. Haier, Role of tumor cell adhesion and migration in organ-specific metastasis formation, Oncology Research and Treatment, 27 (2004) 577-582.
[110] E.T. Roussos, J.S. Condeelis, A. Patsialou, Chemotaxis in cancer, Nature Reviews Cancer, 11 (2011) 573-587.
[111] D.R. Welch, D.R. Hurst, Defining the hallmarks of metastasis, Cancer research, 79 (2019) 3011-3027.
[112] P.S. Steeg, Tumor metastasis: mechanistic insights and clinical challenges, Nature medicine, 12 (2006) 895-904.
[113] M. Poudineh, M. Labib, S. Ahmed, L.M. Nguyen, L. Kermanshah, R.M. Mohamadi, E.H. Sargent, S.O. Kelley, Profiling functional and biochemical phenotypes of circulating tumor cells

using a two‐dimensional sorting device, Angewandte Chemie International Edition, 56 (2017) 163-168.
[114] H. Zou, W. Yue, W.-K. Yu, D. Liu, C.-C. Fong, J. Zhao, M. Yang, Microfluidic platform for studying chemotaxis of adhesive cells revealed a gradient-dependent migration and acceleration of cancer stem cells, Analytical chemistry, 87 (2015) 7098-7108.
[115] Y. Liu, W. Zhao, R. Cheng, J. Hodgson, M. Egan, C.N.C. Pope, P.G. Nikolinakos, L. Mao, Simultaneous biochemical and functional phenotyping of single circulating tumor cells using ultrahigh throughput and recovery microfluidic devices, Lab on a Chip, 21 (2021) 3583-3597.
[116] Y. Lu, S. Yue, M. Liang, T. Wang, R. Wang, Z. Chen, J. Fang, Establishment of a cascaded microfluidic single cell analysis system for molecular and functional heterogeneity analysis of circulating tumor cells, Sensors and Actuators B: Chemical, (2023) 134174.
[117] Y.-C. Chen, S.G. Allen, P.N. Ingram, R. Buckanovich, S.D. Merajver, E. Yoon, Single-cell migration chip for chemotaxis-based microfluidic selection of heterogeneous cell populations, Scientific reports, 5 (2015) 1-13.
[118] Y. Zhang, W. Zhang, L. Qin, Mesenchymal‐mode migration assay and antimetastatic drug screening with high‐throughput microfluidic channel networks, Angewandte Chemie, 126 (2014) 2376-2380.
[119] W. Saadi, S.-J. Wang, F. Lin, N.L. Jeon, A parallel-gradient microfluidic chamber for quantitative analysis of breast cancer cell chemotaxis, Biomedical microdevices, 8 (2006) 109-118.
[120] J. Kim, R.J. DeBerardinis, Mechanisms and Implications of Metabolic Heterogeneity in Cancer, Cell Metabolism, 30 (2019) 434-446.
[121] Y. Gong, P. Ji, Y.-S. Yang, S. Xie, T.-J. Yu, Y. Xiao, M.-L. Jin, D. Ma, L.-W. Guo, Y.-C. Pei, Metabolic-pathway-based subtyping of triple-negative breast cancer reveals potential therapeutic targets, Cell metabolism, 33 (2021) 51-64. e59.
[122] H. Kang, H. Kim, S. Lee, H. Youn, B. Youn, Role of metabolic reprogramming in epithelial–mesenchymal transition (EMT), International Journal of Molecular Sciences, 20 (2019) 2042.
[123] S.C. Schwager, J.A. Mosier, R.S. Padmanabhan, A. White, Q. Xing, L.A. Hapach, P.V. Taufalele, I. Ortiz, C.A. Reinhart-King, Link between glucose metabolism and epithelial-to-mesenchymal transition drives triple-negative breast cancer migratory heterogeneity, iScience, 25 (2022) 105190.
[124] C. van den Hoogen, G. van der Horst, H. Cheung, J.T. Buijs, J.M. Lippitt, N. Guzmán-Ramírez, F.C. Hamdy, C.L. Eaton, G.N. Thalmann, M.G. Cecchini, High aldehyde dehydrogenase activity identifies tumor-initiating and metastasis-initiating cells in human prostate cancer, Cancer research, 70 (2010) 5163-5173.
[125] D. Feng, H. Li, T. Xu, F. Zheng, C. Hu, X. Shi, G. Xu, High-throughput single cell metabolomics and cellular heterogeneity exploration by inertial microfluidics coupled with pulsed electric field-induced electrospray ionization-high resolution mass spectrometry, Analytica Chimica Acta, 1221 (2022) 340116.
[126] C.W. Pan, D.G. Horvath, S. Braza, T. Moore, A. Lynch, C. Feit, P. Abbyad, Sorting by interfacial tension (SIFT): label-free selection of live cells based on single-cell metabolism, Lab on a Chip, 19 (2019) 1344-1351.
[127] C. Zielke, C.W. Pan, A.J. Gutierrez Ramirez, C. Feit, C. Dobson, C. Davidson, B. Sandel, P. Abbyad, Microfluidic Platform for the Isolation of Cancer-Cell Subpopulations Based on Single-Cell Glycolysis, Analytical chemistry, 92 (2020) 6949-6957.
[128] M. Dhar, J.N. Lam, T. Walser, S.M. Dubinett, M.B. Rettig, D. Di Carlo, Functional profiling of circulating tumor cells with an integrated vortex capture and single-cell protease activity assay, Proceedings of the National Academy of Sciences, 115 (2018) 9986-9991.

[129] W.-C. Lee, L. Diao, J. Wang, J. Zhang, E.B. Roarty, S. Varghese, C.-W. Chow, J. Fujimoto, C. Behrens, T. Cascone, Multiregion gene expression profiling reveals heterogeneity in molecular subtypes and immunotherapy response signatures in lung cancer, Modern Pathology, 31 (2018) 947-955.
[130] R.A. Burrell, N. McGranahan, J. Bartek, C. Swanton, The causes and consequences of genetic heterogeneity in cancer evolution, Nature, 501 (2013) 338-345.
[131] N. McGranahan, C. Swanton, Biological and Therapeutic Impact of Intratumor Heterogeneity in Cancer Evolution, Cancer Cell, 27 (2015) 15-26.
[132] Y.P. Yu, D. Landsittel, L. Jing, J. Nelson, B. Ren, L. Liu, C. McDonald, R. Thomas, R. Dhir, S. Finkelstein, Gene expression alterations in prostate cancer predicting tumor aggression and preceding development of malignancy, Journal of clinical oncology, 22 (2004) 2790-2799.
[133] M. Ma, H. Zhu, C. Zhang, X. Sun, X. Gao, G. Chen, “Liquid biopsy”—ctDNA detection with great potential and challenges, Annals of translational medicine, 3 (2015).
[134] C. Alix-Panabières, K. Pantel, Clinical applications of circulating tumor cells and circulating tumor DNA as liquid biopsy, Cancer discovery, 6 (2016) 479-491.
[135] S.L. Kong, X. Liu, S.J. Tan, J.A. Tai, L.Y. Phua, H.M. Poh, T. Yeo, Y.W. Chua, Y.X. Haw, W.H. Ling, Complementary sequential circulating tumor cell (CTC) and cell-free tumor DNA (ctDNA) profiling reveals metastatic heterogeneity and genomic changes in lung cancer and breast cancer, Frontiers in Oncology, 11 (2021) 698551.
[136] K. Gorges, L. Wiltfang, T.M. Gorges, A. Sartori, L. Hildebrandt, L. Keller, B. Volkmer, S. Peine, A. Babayan, I. Moll, Intra-patient heterogeneity of circulating tumor cells and circulating tumor DNA in blood of melanoma patients, Cancers, 11 (2019) 1685.
[137] J.J. Chabon, A.D. Simmons, A.F. Lovejoy, M.S. Esfahani, A.M. Newman, H.J. Haringsma, D.M. Kurtz, H. Stehr, F. Scherer, C.A. Karlovich, Circulating tumour DNA profiling reveals heterogeneity of EGFR inhibitor resistance mechanisms in lung cancer patients, Nature communications, 7 (2016) 1-15.
[138] E. Heitzer, I.S. Haque, C.E. Roberts, M.R. Speicher, Current and future perspectives of liquid biopsies in genomics-driven oncology, Nature Reviews Genetics, 20 (2019) 71-88.
[139] S. Anfossi, A. Babayan, K. Pantel, G.A. Calin, Clinical utility of circulating non-coding RNAs—an update, Nature reviews Clinical oncology, 15 (2018) 541-563.
[140] R. Xu, A. Rai, M. Chen, W. Suwakulsiri, D.W. Greening, R.J. Simpson, Extracellular vesicles in cancer—implications for future improvements in cancer care, Nature reviews Clinical oncology, 15 (2018) 617-638.
[141] K. Gardner, R. Joshi, M.N. Hasan Kashem, T.Q. Pham, Q. Lu, W. Li, Label free identification of different cancer cells using deep learning-based image analysis, APL Machine Learning, 1 (2023).
[142] E. Willms, C. Cabañas, I. Mäger, M.J. Wood, P. Vader, Extracellular vesicle heterogeneity: subpopulations, isolation techniques, and diverse functions in cancer progression, Frontiers in immunology, 9 (2018) 738.
[143] T. Vagner, A. Chin, J. Mariscal, S. Bannykh, D.M. Engman, D. Di Vizio, Protein composition reflects extracellular vesicle heterogeneity, Proteomics, 19 (2019) 1800167.
[144] I. Dagogo-Jack, A.T. Shaw, Tumour heterogeneity and resistance to cancer therapies, Nature reviews Clinical oncology, 15 (2018) 81-94.
[145] K. Hosseini, A. Frenzel, E. Fischer-Friedrich, EMT changes actin cortex rheology in a cell-cycle-dependent manner, Biophysical Journal, 120 (2021) 3516-3526.
[146] J.M. Hope, M.R. Bersi, J.A. Dombroski, A.B. Clinch, R.S. Pereles, W.D. Merryman, M.R. King, Circulating prostate cancer cells have differential resistance to fluid shear stress-induced cell death, Journal of cell science, 134 (2021) jcs251470.
[147] P. Osmulski, D. Mahalingam, M.E. Gaczynska, J. Liu, S. Huang, A.M. Horning, C.M. Wang, I.M. Thompson, T.H.M. Huang, C.L. Chen, Nanomechanical biomarkers of single

circulating tumor cells for detection of castration resistant prostate cancer, The Prostate, 74 (2014) 1297-1307.
[148] P.A. Osmulski, A. Cunsolo, M. Chen, Y. Qian, C.-L. Lin, C.-N. Hung, D. Mahalingam, N.B. Kirma, C.-L. Chen, J.A. Taverna, Contacts with macrophages promote an aggressive nanomechanical phenotype of circulating tumor cells in prostate cancer, Cancer research, 81 (2021) 4110-4123.
[149] S. Tayama, T. Motohara, D. Narantuya, C. Li, K. Fujimoto, I. Sakaguchi, H. Tashiro, H. Saya, O. Nagano, H. Katabuchi, The impact of EpCAM expression on response to chemotherapy and clinical outcomes in patients with epithelial ovarian cancer, Oncotarget, 8 (2017) 44312.
[150] P. Wulfing, J. Borchard, H. Buerger, S. Heidl, K.S. Zanker, L. Kiesel, B. Brandt, HER2-positive circulating tumor cells indicate poor clinical outcome in stage I to III breast cancer patients, Clinical Cancer Research, 12 (2006) 1715-1720.
[151] W. Onstenk, J.-W. Gratama, J. Foekens, S. Sleijfer, Towards a personalized breast cancer treatment approach guided by circulating tumor cell (CTC) characteristics, Cancer treatment reviews, 39 (2013) 691-700.
[152] V. Bozionellou, D. Mavroudis, M. Perraki, S. Papadopoulos, S. Apostolaki, E. Stathopoulos, A. Stathopoulou, E. Lianidou, V. Georgoulias, Trastuzumab administration can effectively target chemotherapy-resistant cytokeratin-19 messenger RNA–positive tumor cells in the peripheral blood and bone marrow of patients with breast cancer, Clinical Cancer Research, 10 (2004) 8185-8194.
[153] V. Georgoulias, V. Bozionelou, S. Agelaki, M. Perraki, S. Apostolaki, G. Kallergi, K. Kalbakis, A. Xyrafas, D. Mavroudis, Trastuzumab decreases the incidence of clinical relapses in patients with early breast cancer presenting chemotherapy-resistant CK-19mRNA-positive circulating tumor cells: results of a randomized phase II study, Annals of oncology, 23 (2012) 1744-1750.
[154] M. Scaltriti, P. Nuciforo, I. Bradbury, J. Sperinde, D. Agbor-Tarh, C. Campbell, A. Chenna, J. Winslow, V. Serra, J.L. Parra, High HER2 expression correlates with response to the combination of lapatinib and trastuzumab, Clinical cancer research, 21 (2015) 569-576.
[155] H.I. Scher, R.P. Graf, N.A. Schreiber, B. McLaughlin, A. Jendrisak, Y. Wang, J. Lee, S. Greene, R. Krupa, D. Lu, Phenotypic heterogeneity of circulating tumor cells informs clinical decisions between AR signaling inhibitors and taxanes in metastatic prostate cancer, Cancer research, 77 (2017) 5687-5698.
[156] J.-H. Cha, L.-C. Chan, C.-W. Li, J.L. Hsu, M.-C. Hung, Mechanisms controlling PD-L1 expression in cancer, Molecular cell, 76 (2019) 359-370.
[157] X. Wang, F. Teng, L. Kong, J. Yu, PD-L1 expression in human cancers and its association with clinical outcomes, OncoTargets and therapy, (2016) 5023-5039.
[158] M. Kowanetz, W. Zou, S.N. Gettinger, H. Koeppen, M. Kockx, P. Schmid, E.E. Kadel III, I. Wistuba, J. Chaft, N.A. Rizvi, Differential regulation of PD-L1 expression by immune and tumor cells in NSCLC and the response to treatment with atezolizumab (anti–PD-L1), Proceedings of the National Academy of Sciences, 115 (2018) E10119-E10126.
[159] R. Said, J. Hernández‐Losa, A. Derouiche, T. Moline, R.S.L. de Haro, S. Zouari, A. Blel, S. Rammeh, S. Ouerhani, Correlation between E‐cadherin/β‐catenin, Vimentin expression, clinicopathologic features and drug resistance prediction in naïve prostate cancer: A molecular and clinical study, genesis, 62 (2024) e23543.
[160] X. Chen, Y. Wang, H. Xia, Q. Wang, X. Jiang, Z. Lin, Y. Ma, Y. Yang, M. Hu, Loss of E-cadherin promotes the growth, invasion and drug resistance of colorectal cancer cells and is associated with liver metastasis, Molecular biology reports, 39 (2012) 6707-6714.

[161] S. Wu, Y. Du, J. Beckford, H. Alachkar, Upregulation of the EMT marker vimentin is associated with poor clinical outcome in acute myeloid leukemia, Journal of translational medicine, 16 (2018) 1-9.
[162] C.H. Stuelten, C.A. Parent, D.J. Montell, Cell motility in cancer invasion and metastasis: insights from simple model organisms, Nature Reviews Cancer, 18 (2018) 296-312.
[163] C.D. Paul, P. Mistriotis, K. Konstantopoulos, Cancer cell motility: lessons from migration in confined spaces, Nature reviews cancer, 17 (2017) 131-140.
[164] C.L. Yankaskas, K.N. Thompson, C.D. Paul, M.I. Vitolo, P. Mistriotis, A. Mahendra, V.K. Bajpai, D.J. Shea, K.M. Manto, A.C. Chai, A microfluidic assay for the quantification of the metastatic propensity of breast cancer specimens, Nature biomedical engineering, 3 (2019) 452-465.
[165] C. Guo, A. Sharp, B. Gurel, M. Crespo, I. Figueiredo, S. Jain, U. Vogl, J. Rekowski, M. Rouhifard, L. Gallagher, Targeting myeloid chemotaxis to reverse prostate cancer therapy resistance, Nature, 623 (2023) 1053-1061.
[166] E.A. Zaal, C.R. Berkers, The influence of metabolism on drug response in cancer, Frontiers in oncology, 8 (2018) 500.
[167] L. Keller, K. Pantel, Unravelling tumour heterogeneity by single-cell profiling of circulating tumour cells, Nature Reviews Cancer, 19 (2019) 553-567.
[168] J. Ferlay, M. Colombet, I. Soerjomataram, D.M. Parkin, M. Piñeros, A. Znaor, F. Bray, Cancer statistics for the year 2020: An overview, International journal of cancer, 149 (2021) 778-789.

Data Availability -

Data will be available upon request from the corresponding author.